NAVAL POSTGRADUATE SCHOOL
Monterey, California

THESIS

NUMERICAL AND EXPERIMENTAL STUDY OF THE PERFORMANCE OF A DROP-SHAPED PIN FIN HEAT EXCHANGER

by

Jihed Boulares

June 2003

Thesis Advisor: Ashok Gopinath

THIS PAGE INTENTIONALLY LEFT BLANK

REPORT DOCUMENTATION PAGE			Form Approved OMB No. 0704-0188
Public reporting burden for this collection of information is estimated to average 1 hour per response, including the time for reviewing instruction, searching existing data sources, gathering and maintaining the data needed, and completing and reviewing the collection of information. Send comments regarding this burden estimate or any other aspect of this collection of information, including suggestions for reducing this burden, to Washington headquarters Services, Directorate for Information Operations and Reports, 1215 Jefferson Davis Highway, Suite 1204, Arlington, VA 22202-4302, and to the Office of Management and Budget, Paperwork Reduction Project (0704-0188) Washington DC 20503.			
1. AGENCY USE ONLY *(Leave blank)*	**2. REPORT DATE** June 2003	**3. REPORT TYPE AND DATES COVERED** Master's Thesis	
4. TITLE AND SUBTITLE: Numerical And Experimental Study Of The Performance Of A Drop-Shaped Pin Fin Heat Exchanger			**5. FUNDING NUMBERS**
6. AUTHOR(S) Jihed Boulares			
7. PERFORMING ORGANIZATION NAME(S) AND ADDRESS(ES) Naval Postgraduate School Monterey, CA 93943-5000			**8. PERFORMING ORGANIZATION REPORT NUMBER**
9. SPONSORING /MONITORING AGENCY NAME(S) AND ADDRESS(ES) N/A			**10. SPONSORING/MONITORING AGENCY REPORT NUMBER**
11. SUPPLEMENTARY NOTES The views expressed in this thesis are those of the author and do not reflect the official policy or position of the Department of Defense or the U.S. Government.			
12a. DISTRIBUTION / AVAILABILITY STATEMENT Approved for public release; distribution is unlimited.			**12b. DISTRIBUTION CODE**

13. ABSTRACT *(maximum 200 words)*

This research presents the results of a combined numerical and experimental study of heat transfer and pressure drop behavior in a compact heat exchanger (CHE) designed with drop-shaped pin fins. A numerical study using ANSYS was first conducted to select the optimum pin shape and configuration for the CHE. This was followed by an experimental study to validate the numerical model.

The results indicate that the drop shaped pin fins yield a considerable improvement in heat transfer compared to circular pin fins for the same pressure drop characteristics. This improvement is mainly due to the increased wetted surface area of the drop pins, and the delay in the flow separation as it passes the more streamlined drop shaped pin fins. The data and conclusions of this study can be used in heat exchanger design for large heat flux cooling applications as in gas turbine blades, and high-power electronics.

14. SUBJECT TERMS Pin-Fin Array, Compact Heat Exchanger, drop-shaped pin fins, Heat Transfer, pressure drop, Micro Heat Exchanger, Turbine Blade Cooling, high power electronics cooling.			**15. NUMBER OF PAGES** 91
			16. PRICE CODE
17. SECURITY CLASSIFICATION OF REPORT Unclassified	**18. SECURITY CLASSIFICATION OF THIS PAGE** Unclassified	**19. SECURITY CLASSIFICATION OF ABSTRACT** Unclassified	**20. LIMITATION OF ABSTRACT** UL

NSN 7540-01-280-5500 Standard Form 298 (Rev. 2-89)
Prescribed by ANSI Std. 239-18

THIS PAGE INTENTIONALLY LEFT BLANK

NUMERICAL AND EXPERIMENTAL STUDY OF THE PERFORMANCE OF A DROP-SHAPED PIN FIN HEAT EXCHANGER

Jihed Boulares
Lieutenant Junior Grade, Tunisian Navy
B.S.M.E., Tunisian Naval Academy, 1999

Submitted in partial fulfillment of the
requirements for the degree of

MECHANICAL ENGINEER

and

MASTER OF SCIENCE IN MECHANICAL ENGINEERING

from the

NAVAL POSTGRADUATE SCHOOL
June 2003

Author: Jihed Boulares

Approved by: Ashok Gopinath
Thesis Advisor

Young W. Kwon
Chairman, Department of Mechanical Engineering

THIS PAGE INTENTIONALLY LEFT BLANK

ABSTRACT

This research presents the results of numerical and experimental study of heat transfer and pressure drop in heat exchanger that is designed with drop-shaped pin fins. The heat exchanger used for this research consists of a rectangular duct fitted with drop shaped pin fins, and is heated from the upper and lower plates. A numerical study using ANSYS was first conducted to select the optimum pin shape and the compact heat exchanger (CHE) configuration. Specifically, the pin shape and the CHE configuration were designed to maximize the heat transfer and minimize the pressure drop across the heat exchanger. After this design work, an experimental study was conducted later to validate the numerical model.

The results indicate that the drop shaped pin fins yield a considerable improvement in heat transfer compared to circular pin fins for the same pressure drop characteristics. This improvement is mainly due to the increased wetted surface area of the drop pins, and the delay in the flow separation as it passes the more streamlined drop shaped pin fins.

The data and conclusions of this study can be applied to the design of gas turbine blades, especially blades that operate at extremely high temperatures. It can also be used in the design of electronic components. This study also demonstrated that numerical models backed with experimental analysis can reduce both the time and money required to create and evaluate engineering concepts, especially those that deal with fluid flow and heat transfer.

THIS PAGE INTENTIONALLY LEFT BLANK

TABLE OF CONTENTS

LIST OF FIGURES

LIST OF TABLES

THIS PAGE INTENTIONALLY LEFT BLANK

ACKNOWLEDGMENTS

I would like to extend sincere thanks and gratitude to Professor Ashok Gopinath for his guidance and assistance throughout this research. I would also like to thank CDR Len Hamilton for his direction in learning the ANSYS software, LT David Ramthun for developing the experimental apparatus and LT Jeffrey Summers for his help and friendship. Finally, I would like to thank my parents for their encouragement through the years and my girlfriend, Andrea, for her moral support and motivation.

THIS PAGE INTENTIONALLY LEFT BLANK

I. INTRODUCTION

Heat exchangers have been widely studied as one of the most fundamental applications of heat transfer and fluid mechanics. Of these compact heat exchangers (which have a large area density) have seen growing use in a variety of fields such as in gas turbine cooling, electronics cooling and other applications that call for large heat flux removal rates. One of the most common designs in these applications use an enclosed pin fin heat exchanger duct flow configuration with pins of round cross section. Other pin fin shapes have received limited attention. Round pin fins have the disadvantage of early flow separation over the fin, which lowers the heat transfer and increases the total pressure drop across the heat exchanger. When looking to improve the performance of these heat exchangers, one particular area of interest lies in using different pin shapes that are able to delay flow separation. Some studies investigated oblong (Arora) and elliptical shapes (Chen, Z., Li, Q., Flechtner, U., and Warnecke,1997).

A thorough experimental characterization of different possible shapes is a very expensive and time consuming task, due to the enormous cost of experimental parts and tools. In addition, there is little geometric flexibility built into test models, and a new model has to be constructed for each different configuration. Numerical study can be the remedy for that by offering a quick and cost effective means of study with the advantage of having great flexibility in the geometry and boundary conditions. Many configurations can be studied at different Reynolds

numbers and turbulence levels, and many different pin shapes and arrangements can be investigated. After selecting an optimum heat exchanger design based on numerical study, an experiment can be conducted on a far narrower range of options to validate the predicted performance of the heat exchanger design.

II. BACKGROUND AND OBJECTIVE

A. COMPACT HEAT EXCHANGERS (CHE)

Compact heat exchangers can be defined as heat exchangers characterized by a high wetted surface area (heat transfer area) per unit volume. This ratio should be typically higher than $600-700\ m^2/m^3$ for the heat exchanger to be treated as compact (Shah & Kraus,1990), whereas for typical industrial shell and tube heat exchangers this ratio goes down to less than $100 m^2/m^3$. Making the heat exchanger compact has the advantage of reducing space, weight, cost, energy required, in addition to the high heat transfer per unit footprint area it affords. Examples for CHE are a bundle of very small-diameter tubes for both high and low-density fluids, circular tubes with extended surfaces or circular fins attached to the outside, stack of flat plates placed very close together and compact matrix constructed using stacks of plates and fins or packed bundle of tubes frequently used in liquid to gas exchangers.

Compact heat exchangers have a major role in the development of light cheap and efficient heat exchangers used for aerospace, marine transportation system, air conditioning and refrigeration applications.

B. MOTIVATION FOR CHE STUDY

Lately compact heat exchangers have been the subject of extensive research (Kays and London, 19xx, Shah et al., 2001) because of their importance in a wide variety of

engineering applications. One of the most important new applications is in cooling electronic components to keep them functioning efficiently and increase their life expectancy. Another application is in modern high performance gas turbine engines operating at high turbine inlet temperature. For these types of engines, performance and efficiency increases as we increase the inlet temperature, which is limited to the temperature the metal can withstand. The engine components exposed to the hot gas flow are required to be cooled, in particular at the leading edge of the gas turbine blades. In addition, an enforced structure is required at that critical location of the blade. Internal cooling air for each blade is supplied from the engine compressor at the cost of the cycle efficiency. So the design problem consists of having a high efficiency heat exchanger with high heat transfer, and small pressure drop. One of the proposed solutions to this design problem is to have a small shroud enclosed ducted heat exchanger with staggered arrays of pin fins with air in cross flow over the pins.

C. PAST CONTRIBUTIONS

Many studies have been conducted on this topic including the experimental studies of VanFossen (1982) which investigated the Heat transfer coefficients for staggered arrays of short pin fins, Metzger et al (1982) who studied the developing heat transfer in rectangular ducts with staggered arrays of short pin fins, Yao Peng (1984) who studied the heat transfer and friction loss characteristics of pin fins cooling configurations, Chyu and Goldstein (1991) who used the mass transfer analogy to study the influence of an array of wall-mounted cylinders

on the heat transfer from flat surfaces. Other issues concerning this type of heat exchanger investigated include the effect of the thermal boundary conditions, pin fin configuration, the optimal row spacing for the cross-pin array, the array orientation…

Most of these studies investigated the cylindrical shaped pin fins. Few have studied the effect of different shape pin fins. Arora (1989) studied the pressure drop and heat transfer characteristics of circular and oblong low aspect ratio pin-fins and showed that oblong pin fins with major axis parallel to the flow direction result in higher heat transfer rates and lower friction factor than the circular pin fins but for other orientations oblong pin fins do not offer any significant advantage over the circular ones. Metzger (1984) studied the effects of pin shape and array orientation on heat transfer and pressure loss in pin fin arrays and concluded that the oblong pin array increases the heat transfer about 20% over the round pins but at the same time the pressure loss was doubled. Qingling et al. (1997) evaluated the heat transfer and pressure drop in rectangular channels with elliptic pin fins and concluded that the channel with elliptical pins has higher heat transfer than that with circular pins with less flow resistance but the Nusselt numbers are lower. O'Brien et al (2001) studied the local heat transfer and pressure drop for finned-tube heat exchangers using oval tubes and vortex generators(delta winglets).

All these studies were experimental studies that cost much money due to the large cost of tools and parts needed, the considerable resources required to set up the

experiment and run it, and the inflexibility from the point of view of geometry and boundary conditions.

Only recently has numerical modeling shown greater promise with the advent of advanced computers and software. Numerical modeling has the advantage of offering a cost and time effective model with flexible geometry and boundary conditions. However even numerically it is important to be true to the physics and have flow models that capture the flow behavior accurately.

D. CURRENT OBJECTIVE

The main objective of this work is to develop a reliable three dimensional numerical model of a compact heat exchanger consisting of a rectangular duct with staggered arrays of drop-shaped pin fins in a cross flow of air, and characterize the heat transfer and associated pressure drop behavior. Stream wise and span wise spacing effects, as well as pin tail elongation will be investigated, and an optimum geometric configuration together with a pin shape will be selected based on the overall heat exchanger performance. A comparison between pressure drop and heat transfer for round pins CHE and drop shaped pins CHE will be carried out. Finally, a brief experimental study will be carried out to gather empirical data to evaluate the accuracy of the numerical work.

III. MODELING

A. NUMERICAL MODEL

1. Physical Model of CHE

In this study, the compact heat exchanger domain consists of 10 rows of staggered drop shaped cross-pins with axes perpendicular to the flow, as shown in Figure 1. The main geometrical dimensions that characterize the heat exchanger are the pin height (H), the diameter of the cylindrical portion of the pin (D), the streamwise pin spacing (X), the spanwise pin spacing (S) and the pin-tail length (L). The streamwise pin spacing (X) was kept constant at a value equal to 12.7 mm (consistent with what Metzger (1982) used in his study) and was considered as a reference length scale. The heat exchanger is composed of a rectangular duct having 10X as length, 5S as width and H as height together with a bank of 45 solid pins that span the end walls. Many different arrangements were investigated by changing the X/D, S/D, and L/D ratios.

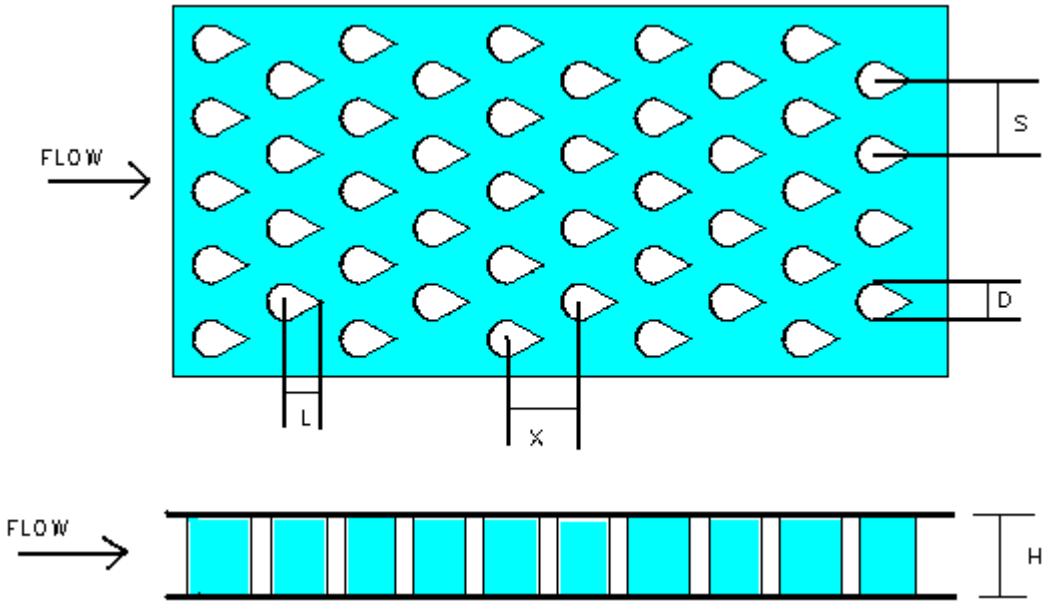

Figure 1. Staggered pin-fin array

2. Pin-Fin Geometry

Most of the recent research has concentrated on circular pin fins probably because they are easy to manufacture. However, it is by no means clear that circular pin fins have the highest heat transfer or the lowest pressure drop. It is clear that cylinders with elliptic shaped cross section have lower resistance to the flow and lower friction factor than the circular ones, as well as a higher surface wetted area that can increase the heat transfer.

In this study, a drop shaped pin fin is selected to improve the heat transfer and the pressure loss. The configuration of the pin is shown in Figure 2. Its cross section consists of a circular leading edge that extends along $90+2\times\alpha$ deg and a triangular trailing edge. The triangle edges are tangent to the circular arc.

The distance between the center of the circle and the triangle apex is L. Having the triangular portion of the pin will help increase the wetted surface area of the heat exchanger leading to a major increase in the heat transfer and the efficiency. In addition it delays the separation in comparison with the circular cross section which helps decrease the friction factor and the flow resistance leading to a major decrease in the pressure loss.

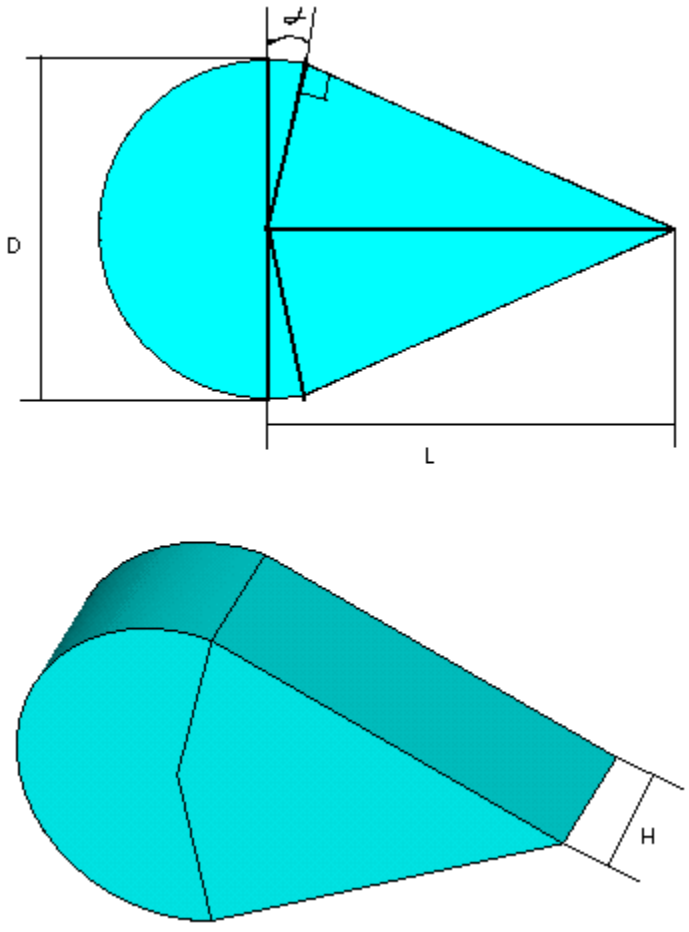

Figure 2. Pin shape and dimensions.

3. Numerical Model

The finite element modeling was conducted using the FLOTRAN solver of the engineering simulation software ANSYS version 6.0. This study examined laminar flow (for low Reynolds numbers), turbulent Flow (for high Reynolds numbers) and heat transfer characteristics within a 3-D staggered short drop-shaped pin fin array compact heat exchanger. Taking advantage of the symmetry planes in the heat exchanger, and in order to minimize the computational requirements and time, only one fourth of the heat exchanger was modeled, as shown in Figure 3.

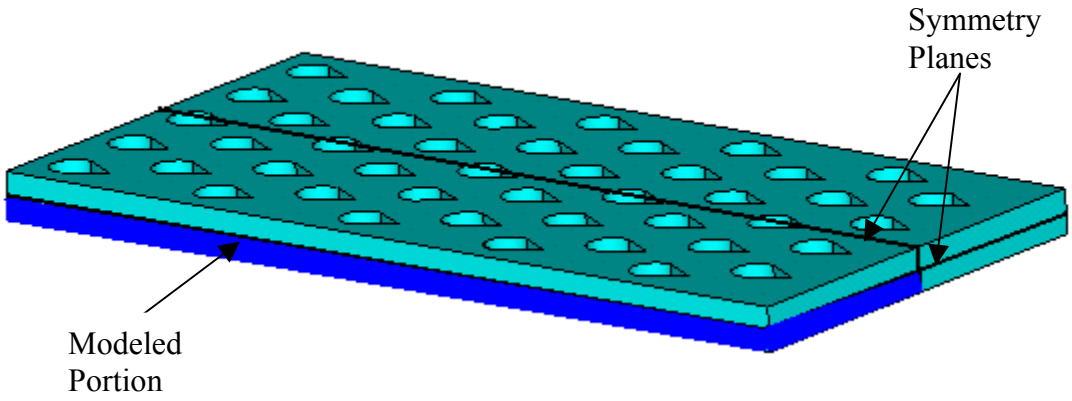

Figure 3. Symmetry planes and CHE model.

Also, to simplify the model and reduce the number of required elements, nodes and time required for the calculation, only the fluid (air) was modeled and the solid walls, as well as, the pins were considered as isothermal boundary conditions eliminating the need to calculate the temperature distribution in the solid pins and the walls. This was especially justifiable for the short pins being considered in this study.

Based on these simplifications, the model appears as shown in Figure 4. The model is composed of three parts. The first part is a smooth entrance duct upstream of the test section having the same cross section as the test section and long enough to provide a fully developed flow condition at the entrance to the heat exchanger. The length of this section varies with Reynolds number. The air then passes through the test section composed of 10 rows of drop shaped pin fins. After the test section the air continues through a smooth 0.125 m exit section design to prevent boundary condition feedback into the test section.

By keeping the pin height H/D=1 and setting S/D and X/D to 1.5,2,3,4, and varying L/D, many configurations could be investigated and the optimum configuration giving the highest heat transfer and the lowest pressure loss could be determined.

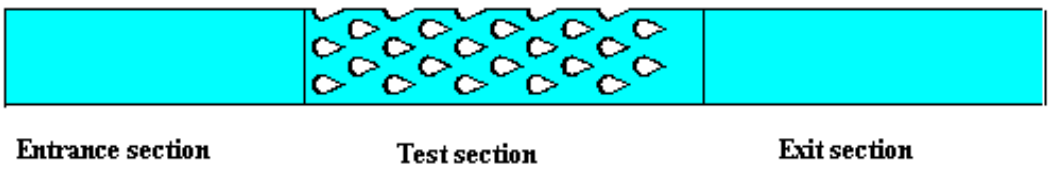

Figure 4. Finite element model

4. Numerical Mesh

To mesh the model, hexahedral 8-node element spacing was specified along the boundary and swept later to cover the entire model volume, as shown in Figure 5. Meshing also was refined in some critical areas to ensure coverage for satisfactory resolution. It was refined near the no slip walls where velocity and temperature gradients were expected to be high, and also between the pins to capture

the flow acceleration due to the decrease in the cross section area. Nodes were also concentrated around the pins to account for the change of the velocity and temperature gradient and pressure drop and at the end wall were the temperature gradients are expected to be higher. Grid independence was always verified. Since the current ANSYS license is limited to 256,000 nodes, two runs were done for each configuration at a certain Reynolds number. The first one was completed at a number of nodes close to 256,000 and the second at approximately 25-30% less nodes. A run was considered to be grid independent, if the overall heat transfer rate difference between the two remained below 2%.

A result was also considered valid if the model outlet temperature matched the calculated outlet temperature using an energy balance method to within 2%.

Finally, the number of solver iterations was selected, so that the difference in the overall heat transfer rate varied by less than 2% between the last 10 iterations.

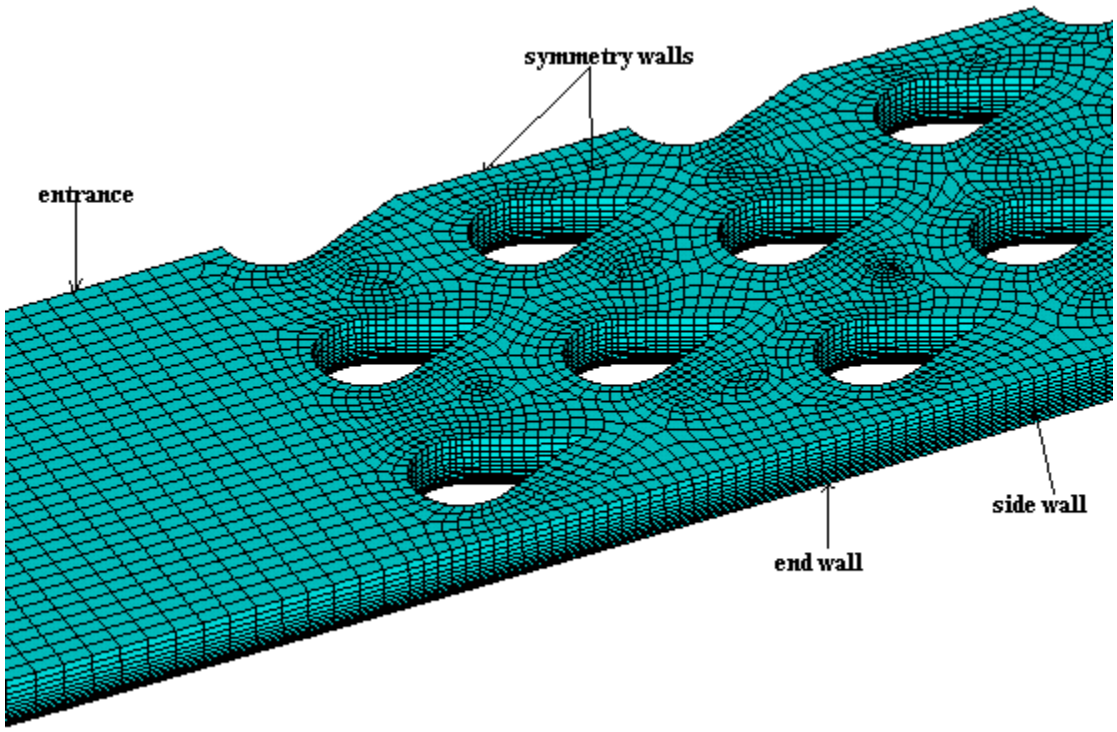

Figure 5. Sample Model meshing (X/D=2,S/D=2,L/D=1.2)

5. Solution Technique

All flows were specified as steady state and incompressible. The standard $k_t - \varepsilon$ turbulence model with Van Driest coupling for the wall region was set for each model. The CFD FOLTRAN solver was set to use the Preconditioned Generalized Minimum Residual (PGMR) method and the Collocated-Galerkin (colg) approach was used to discretize the advection term. More details on these solvers can be found in the ANSYS Theory Reference Manual.

6. Boundary Conditions

a. Pins

The pins are treated as short and with very high thermal conductivity. The pins are therefore assumed to be isothermal with a uniform temperature of 306 K. The no slip condition was applied to the pin surfaces.

b. End Wall

The end wall was kept at a constant temperature of 306 K. Since it is a rigid boundary the no slip condition was applied leading to a zero velocity in the 3 directions, Ux=Uy=Uz=0. The inlet and exit end walls were modeled as adiabatic walls with zero velocity in the three conditions.

c. Symmetry Walls

The symmetry walls are assumed to be adiabatic modeled with zero heat flux. The mid-height plane was given zero velocity in the z direction (Uz=0) and the mid-width plane was given a zero velocity in the y direction (Uy=0) thus preventing the flow from crossing the boundary but yet allowing a velocity profile to develop. The inlet and exit symmetry walls have the same features as in the test section.

d. Side Wall

The sidewall was modeled to be adiabatic with zero heat flux. The no slip condition was applied and zero velocity in the tree direction (Ux=Uy=Uz=0) was used. The inlet and exit sidewalls has the same properties as the same properties as the test section ones.

e. Inlet

The inlet air temperature was set to 300 K. The inlet velocity depends on the chosen Reynolds number, which was set based on the wetted surface area.

Figures 6 and 7 give a clear idea of the boundary conditions implemented.

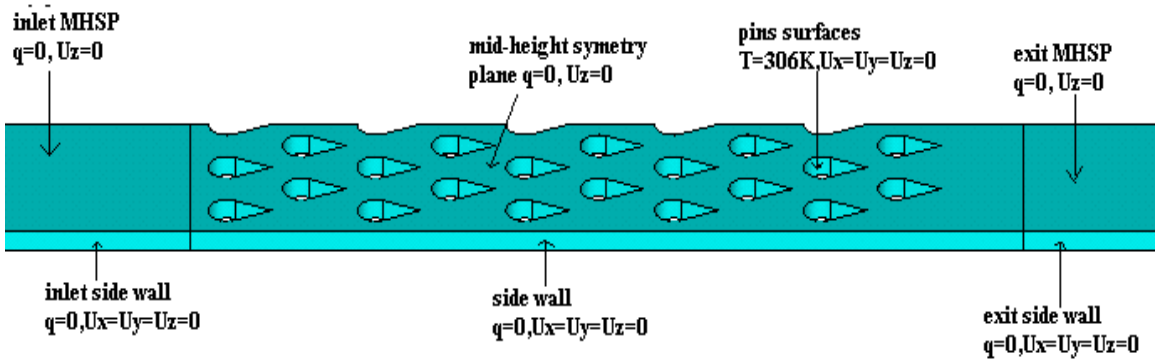

Figure 6. Model's top view with boundary conditions

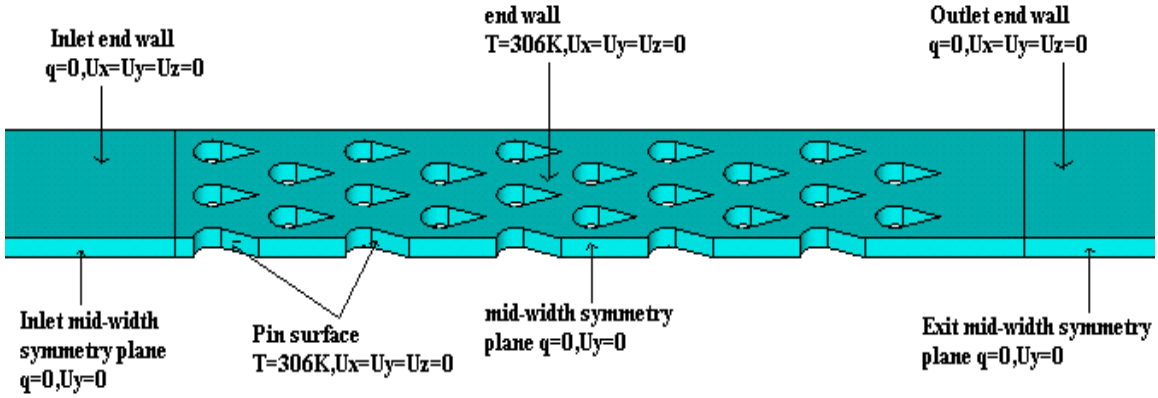

Figure 7. Model's bottom view with boundary conditions

7. Problem Parameters

The total heat transfer rate, mass flow, pressure drop and the outlet bulk temperature are provided as the output of the ANSYS CFD/Flotran results file. The other parameters are calculated as below.

a. Area Wetted

The wetted surface area is defined as the total heat exchanger surface area in contact with the coolant fluid. It includes the upper and lower plates area in contact with the fluid and the pin areas in contact with the fluid.

$$Aw = 2[5S(10x + L) - 45(2L\cos\theta + (\pi + 2\theta)\frac{D}{2})H] + 45[\frac{D}{2}(\pi + 2\theta) + 2L\cos\theta]H \quad (1.1)$$

b. Open Volume

The total volume is defined as the total fluid volume inside the heat exchanger. It is equal to the total heat exchanger internal volume minus the volume occupied by the pins.

$$Vopen = 5SH(10x + L) - 45(\frac{D}{2}L\cos\theta + \pi\frac{D^2}{4}\frac{(\pi + 2\theta)}{2\pi})H \quad (1.2)$$

c. Hydraulic Diameter

The hydraulic diameter was defined as the ratio of the total wetted (heat transfer) surface area to the open duct volume available for flow. This ratio is the most appropriate characteristic length for the heat exchanger, since it is representative of the different configurations investigated in this study and captures the influence of all the length scales in the problem.

$$Dh = \frac{4Vopen}{Aw} \quad (1.3)$$

d. Average Flow Area

The average flow area is defined as

$$\bar{A} = \frac{Vopen}{10x + L} \quad (1.4)$$

e. Reynolds Number

After defining the hydraulic diameter and the average flow are an appropriate Reynolds number will be defined as

$$\mathrm{Re}_{Dh} = \frac{\dot{m} D_h}{\mu \bar{A}} \quad (1.5)$$

f. Outlet Temperature

The outlet temperature was calculated as below using an energy balance across the ends of the heat exchanger. A run was considered valid only if the difference between the calculated and numerical result was found to be less than 0.1 k.

$$T_{out} = T_{in} + \frac{q}{\dot{m} C_p} \quad (1.6)$$

g. Log Mean Temperature Difference

The log mean difference temperature was defined as the "average" driving temperature difference between the hot and cold streams for heat transfer calculations. For heat exchangers, the use of the log mean difference temperature makes the calculation of the heat transfer coefficient more accurate. It is defined as

$$\Delta T_{LM} = \frac{(T_{wall} - T_{coolant_{in}}) - (T_{wall} - T_{coolant_{out}})}{\ln(\frac{T_{wall} - T_{coolant}}{T_{wall} - T_{coolantout}})} \quad (1.7)$$

h. Heat Transfer Coefficient

The heat transfer coefficient was calculated based on the wetted surface area and the log mean temperature difference. It is defined as

$$\overline{h} = \frac{q}{A_{wetted}\Delta T_{LM}} \quad (1.8)$$

$\overline{h}$ Is defined as the heat transfer inside the test section.

i. Nusselt Number

The Nusselt number is calculated as below

$$Nu_{Dh} = \frac{\overline{h}\, D_h}{K} \quad (1.9)$$

j. Friction Factor

The friction coefficient is calculated using this formula

$$f = \frac{2\Delta P D_h}{\rho(10x + L)\overline{U}^2} \quad (1.10)$$

Where

ΔP is the pressure drop inside the test section.

$\overline{U}$ average velocity inside the test section defined as

$$\overline{U} = \frac{\dot{m}}{\rho \overline{A}} \quad (1.11)$$

k. Friction Power E

The friction power is defined as the mechanical energy flux due to pressure drop inside the heat exchanger; in other words, it is the power required by the blower to overcome the friction forces inside the

heat exchanger. The quantity E is defined on the basis of per unit wetted surface area. Together with the heat transfer coefficient the friction power can provide a rational basis for comparing the performance of one configuration against another. The friction power is defined as

$$E = \frac{\dot{m}\Delta P}{\rho A_w} \qquad [\frac{W}{m^2}] \quad (1.12)$$

l. Porosity P

Porosity is defined as the ratio of the open volume to total volume in the heat exchanger.

$$P = \frac{V_{open}}{V_{total}} \quad (1.13)$$

m. Volumetric Heat Transfer Area Density

The volumetric heat transfer area density of a CHE is defined as the ratio of the total wetted surface area to the total CHE volume.

$$\alpha = \frac{A_w}{V_t} \quad (1.14)$$

B. EXPERIMENTAL SET UP

The experimental setup was designed and constructed for a parallel study on round pins (Ramthun, 2003). In the present work, the round pins were replaced with drop shaped pin fins. The particular heat exchanger configuration used in this experiment was X/D=1.5, S/D=1.5 H/D=1, L/D=1.5.

The experimental model consists of

- Inlet section: To minimize friction, the inlet section was designed using half inch thick Plexiglas. The total inlet section was designed

to be 9 ft long to ensure fully developed flow up to Reynolds number of 100,000. The inlet section has a width of 7.5D, which comes to be 250mm (D is the pin diameter, which is equal to 0.033m) and height of D to be consistent with the test section.

- Test section: To achieve a high conductivity for the pins and the end walls, the upper and lower plates as well as the pins of the test section were constructed using 6061 T6 aluminum plate and rods. The sidewalls were constructed with Plexiglas. To achieve the 1-5-1.5-1.5 configuration with a pin diameter of 33mm the test section was given a length of 250mm, a width of 50mm and a height of 33mm. Inside the HE, 10 rows of staggered drop shaped cross-pins where set up with axes perpendicular to the direction of flow. A total of 45 pins were used. The two end walls were heated using twenty 50-watt electrical heaters. A thermocouple was mounted at each heater location to keep the upper and lower plates at a constant temperature.

- Exit duct: The exit section was modeled to match the rectangular exit cross section of the exit test section and the circular cross section of the exit flow straightening section. The exit section was insulated to reduce heat losses.

- Pressure transducer: The inlet pressure tap was mounted at the entrance section just before the test section and the outlet pressure tap was

mounted on the exit duct just after the test section. This provides the pressure drop across the test section as well as the total pressure at the exit to calculate the density.

- Mass flow meter: The mass flow meter (turbine type) was mounted in the exit flow downstream of the test section after a suitable flow straightening duct length.

A simple program using on/off control was written to maintain the endwalls at the specified temperature. The software gave as output the flow meter and the pressure transducer voltages used to calculate the mass flow, the pressure drop inside the heat exchanger and the test section exit temperature. It also gave the inlet temperature and four outlet temperatures, which were averaged to calculate the average outlet temperature. From the data read into an Excel file, the total energy given to the heaters was calculated, which determined the total heat transfer rate. The data acquired was inlet temperature, average outlet temperature, mass flow rate and pressure drop across the array.

For each test series, the first run was carried out under zero airflow to measure heat losses to the environment. The purpose behind this run was to measure the total heat loss from the test section to the environment for calibration purposes. The zero offset voltages of the pressure transducer and the mass flow meter were also recorded at this stage.

Following this calibration run, additional data runs lasting 20 minutes were conducted for each test point. The

data was collected and the results were obtained as shown in the sample calculation in Appendix D.

VI. RESULTS AND DISCUSSION

A. INTRODUCTION

This focus of this study was on investigating the heat transfer and pressure losses inside a drop-shaped pin fin heat exchanger. The hydraulic diameter was selected to be the characteristic length, since it is representative for the different configurations studied. For accuracy reasons, and to take account of the configuration and the pin dimensions variations, the heat transfer coefficient was calculated based on the wetted surface area, and the log mean temperature difference. The Nusselt number was calculated at a later stage based on the heat transfer coefficient and the hydraulic diameter. The friction power was defined based on the wetted surface area and together with the heat transfer was the basis for comparison of the performance of the different configurations (Table 1).

X/D	S/D	L/D
1.5	1.5	0.5-0.75-1-1.25-1.35-1.5-1.75
2	2	0.5-0.75-1-1.5-2-3
3	3	0.5-0.75-1-2-2.5-3-4-5
4	4	0.5-0.75-1-2-3-4-5-6-7
4	2	1-2-3-4-5-6
1.5	4	1.5
3	1.5	1.5
1.5	2.5	1.5

Table 1. Numerical configurations investigated.

A comparison between the round pin and the drop pin heat exchangers was also conducted. The limiting case of a drop pin HE with L/D = 0.5 is a round pin which was also treated to obtain a baseline result.

Results from the different configurations were compared between the heat transfer and friction power and an optimum was selected.

The results are presented below in figures and tables for different values of X/D-S/D-L/D with H/D = 1.

B. NUMERICAL RESULTS

1. Optimum Configuration Based on the HE Size

The first step is to select the optimum configuration based on the HE size. All the configurations mentioned in Table 1 were numerically studied. The optimum pin dimensions for each configuration were first selected, based on heat transfer and pressure drop behavior, and a comparison between the selected HE was conducted. The selected configurations to be compared are

- 1.5-1.5-1.5
- 2-2-3
- 3-3-5
- 4-4-5
- 4-2-5
- 1.5-4-1.5

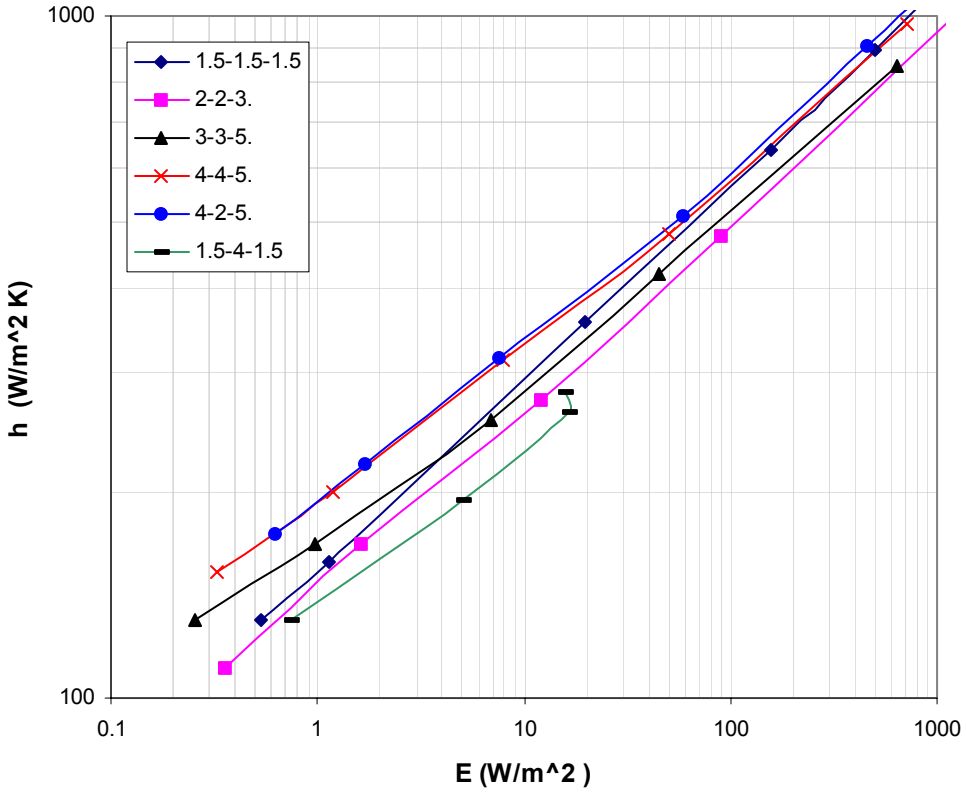

Figure 8. Comparison of the numerical heat transfer coefficient versus the friction power for the different HE configurations.

Figure 8 shows that the 4-4-5 and the 4-2-5 configurations seem to have the highest heat transfer coefficient for the same friction power for all Reynolds numbers in the range of 3000 - 50000.

The 1.5-1.5-1.5 configuration seems to have less heat transfer coefficient for Reynolds number between 3000 and 10000, but after 10000 it converges to the same level as 4-4-5 and 4-2-5 by having almost the same heat transfer coefficient for the same friction power as the best configuration.

To select the best configuration, two factors were considered. First, Figure 8 showed that even though 1.5-1.5-1.5 has less heat transfer coefficient for low Reynolds numbers, it is as efficient as the best configuration starting from a Reynolds number of about 10000. Second, the 1.5-1.5-1.5 setup has a 27% increase in wetted surface area over the 4-4-5 case and 117% over the 4-2-5 case. The last factor makes the 1.5-1.5-1.5 case have higher heat flux than all the other configurations for the same friction power for the entire Reynolds number range. Based on this, the X/D=1.5 S/D=1.5 configuration was selected to be the subject of a thorough numerical study to figure out the best pin dimension for a limited experimental study.

2. Optimum Configuration Based on the Pin Dimensions

Knowing that the S/D=1.5, X/D=1.5 was the optimum configuration among the ones studied, the next task was to select the optimum pin dimension based on the drop tail length that gave the highest heat transfer with as low a pressure drop as possible, and compare it with a similar round pin HE.

a. Friction Factor

The friction factor is a very important property, since it reflects the amount of power needed to "push" the air through the heat exchanger. The friction factor was calculated using the formula (1.10) after determining the pressure drop ΔP from the ANSYS result file. This friction factor is defined on the basis of an equivalent combination of viscous shear (skin friction) and pressure force (form drag).

Figure 8 shows the friction factor versus the Reynolds number (based on the hydraulic diameter) for the configuration 1.5-1.5-1.5 with different pin tail lengths. This figure shows that the round pin heat exchanger (L/D=0.5) has the highest friction factor. As we increase the tail length, the friction factor goes down due to the flow separation delay, which reduces the form drag. The configuration having L/D=1.25 seems to have the lowest friction factor with an improvement of 58% over the round pins. For L/D higher than 1.25, the friction factor tends to go back up but is still lower than the round pins. This increase can probably be explained by the increase in the skin friction caused by the increase in the friction area, as the tail length increases, and at the same time a drop in the rate of decrease of the form drag. Another reason for increase in the friction factor is that increasing the tail length to more than 1.25 causes the pins to overlap thus forcing the flow to follow a more twisted path around the pins which results in an increase in the pressure drop.

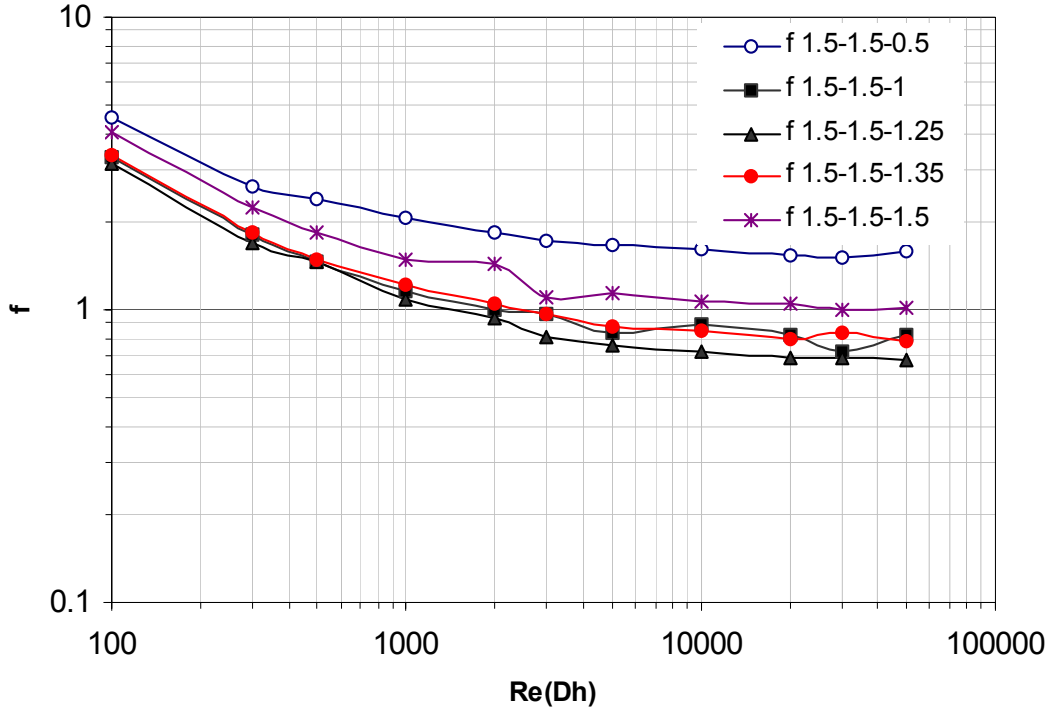

Figure 9. Comparison of the numerical friction factor as a function of Reynolds number for (X/D=S/D=1.5). The open circles are for round pins.

Figure 9 shows that the configuration 1.5-1.5-1.25 is the optimum configuration for all Reynolds numbers. The friction factor decreases to around 58% for the turbulent cases and to about 45% for the laminar cases. The configuration 1.5-1.5-1 and 1.5-1.5-1.35 seem to have a decrease in the friction factor of about 48% in turbulent cases and about 37% for the laminar cases. For the 1.5-1.5-1.5 configuration, there is an improvement of 36% in the turbulent cases and 0.27 to 0.35 in the turbulent cases.

The friction factor was related to the Reynolds number with a power function correlation for each configuration and for the turbulent and laminar cases, as shown in Table 1.

	Configuration	Friction factor
Laminar $\mathrm{Re}_{Dh} = 100 - 1000$	1.5-1.5-0.5	$f = 21.57\,\mathrm{Re}^{-0.351}$
	1.5-1.5-1	$f = 26.455\,\mathrm{Re}^{-0.46}$
	1.5-1.5-1.25	$f = 25.6\,\mathrm{Re}^{-0.4623}$
	1.5-1.5-1.35	$f = 26.39\,\mathrm{Re}^{-0.455}$
	1. 5-1.5-1.5	$f = 29.547\,\mathrm{Re}^{-0.44}$
Turbulent $\mathrm{Re}_{Dh} = 2000 - 50000$	1.5-1.5-0.5	$f = 2.5778\,\mathrm{Re}^{-0.0493}$
	1.5-1.5-1	$f = 1.7418\,\mathrm{Re}^{-0.0766}$
	1.5-1.5-1.25	$f = 1.7318\,\mathrm{Re}^{-0.0913}$
	1.5-1.5-1.35	$f = 1.8424\,\mathrm{Re}^{-0.0818}$
	1.5-1.5-1.5	$f = 2.3591\,\mathrm{Re}^{-0.0818}$

Table 2. Friction factor correlations

b. Nusselt Number

Figure 10 shows a plot of the Nusselt number calculated as defined in equation 1.9 (based on the hydraulic diameter) versus Reynolds number.

Figure 11 shows the Nusselt number also calculated using equation 1.9 but this time based on the pin diameter keeping with the convention of previous studies in the literature.

The first figure shows that the round pins yield a higher heat transfer than the entire drop shaped pins for Reynolds number between 300 to 50000 for the particular sizes being considered. However for the same range of Reynolds numbers the second figure shows that the drop shaped pins give a better Nusselt number than the round pins.

Figure 10 doesn't really give a good idea of the heat transfer because the Nusselt number in this case was based on the hydraulic diameter as in equation 1.9. By changing the pin shape from the round pins to drop shaped pins the hydraulic diameter goes down since from equation 1.5 we can see that the hydraulic diameter is proportional to the open volume and inverse proportional to the wetted surface area. The drop shaped pins have a higher wetted surface area and the CHE made from those pins has a less open volume than the one made by round pins, which allows it to have a smaller hydraulic diameter. As a result the heat transfer coefficient for a drop shaped CHE can increase with a rate smaller than the hydraulic diameter decrease allowing the total Nusselt number to decrease.

Figure 11 gives a better idea of the heat transfer coefficient. Since the diameter is now a constant value equal to the pin diameter, and since the air conductivity is constant, by looking at equation 1.9 for a constant diameter we can realize that the CHE with the highest heat transfer coefficient is the one with the highest Nusselt number.

From figure 11 we can conclude that the 1.5-1.5-1.5 CHE configuration gives the best heat transfer followed

by 1.5-1.5-1.35, 1.5-1.5-1.25, 1.5-1.5-1.25-1.5-1.5-1 and the round pins come at the end with the least heat transfer.

From Figure 11 it can be concluded that the optimum configuration giving the best heat transfer is 1.5-1.5-1.5 but it is clear that the heat transfer behavior alone does not provide a comprehensive assessment of heat exchanger performance. The increased pressure drop incurred must be weighed against the improvements of heat transfer for each pin fin configuration. This optimization process is critical for comparing the contrast between heat exchanger heat transfer and pressure drop gains and losses.

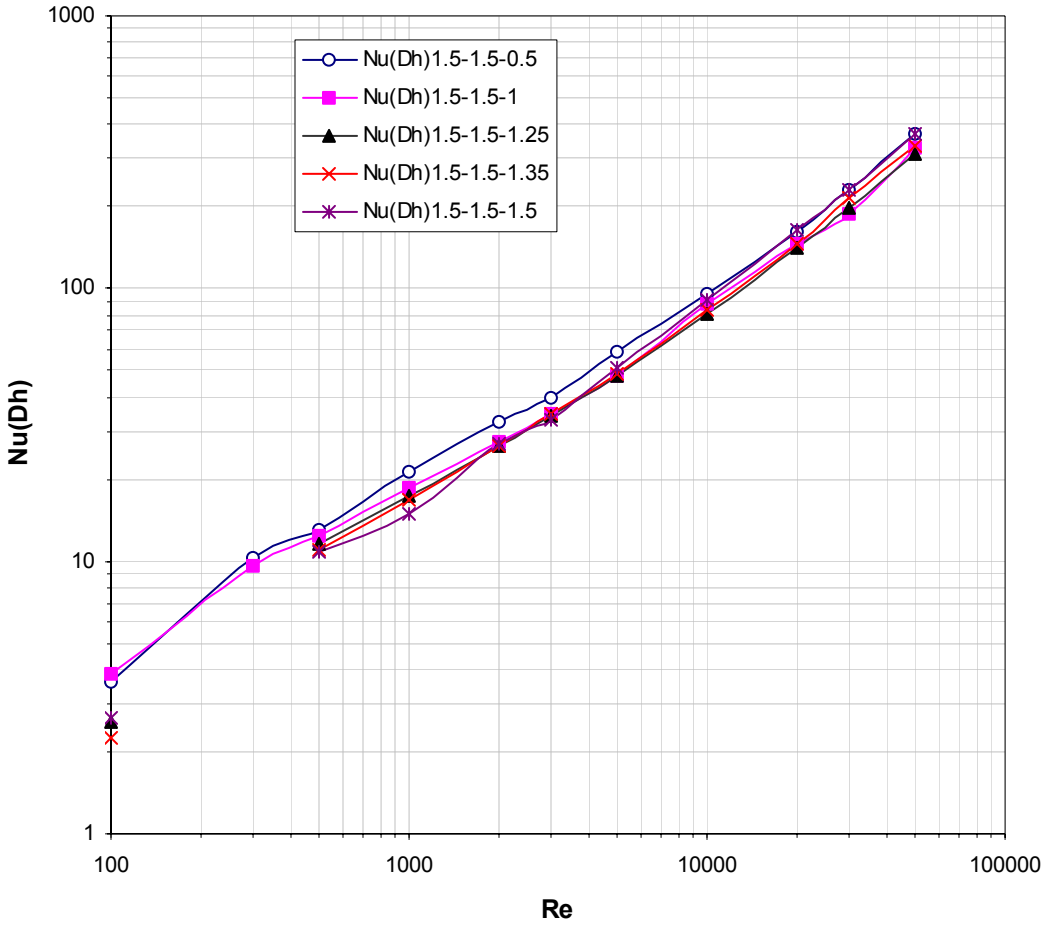

Figure 10. Comparison of the numerical Nusselt number based on hydraulic diameter versus Re (Dh) for X/D=S/D=1.5 and different tail length. Circles are the round pins.

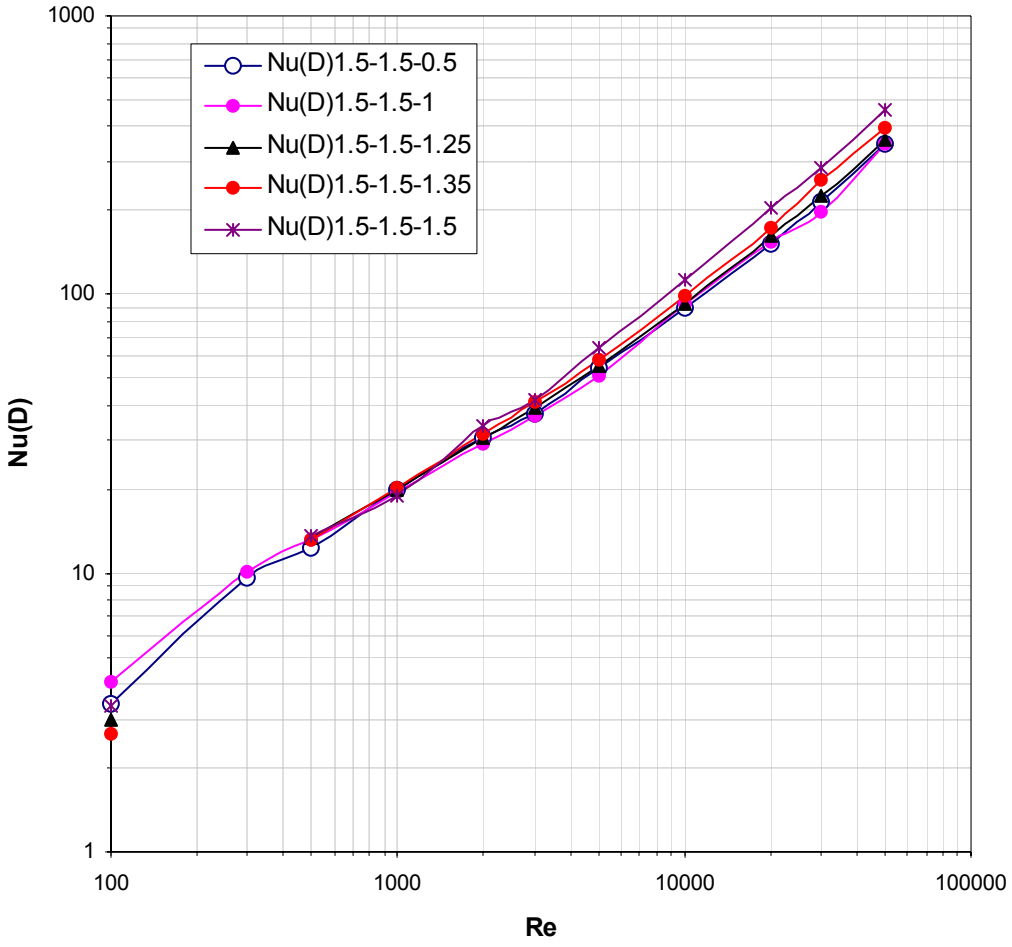

Figure 11. Comparison of the Numerical Nusselt number based on pin diameter versus Re (Dh) for X/D=S/D=1.5 and different tail length. Circles are the round pins.

c. Heat Transfer Coefficient

Figure 12 shows the heat transfer coefficient calculated from formula 1.8 versus the Reynolds number calculated from equation 1.5 for X/D=S/D=1.5 and different tail lengths. From this graph it is clear that the heat transfer coefficient increases as the tail length increases. The configuration designed with L/D=1.5 has the

highest heat transfer coefficient followed by L/D=1.35, L/D=1.25,L/d=1 and last one comes the round pin with the lowest heat transfer coefficient. The enhancement of heat transfer coefficient between the round pin and the drop pin heat exchanger is about 34.48% for Re=5000, 33.35% for Re=30000, 35% for Re=20000, 26% for Re=10000, 18% for Re=5000, and 12% for Re=3000. The reason for this improvement can be drown from figure 12 and 13.

Two runs were done, one of them for a heat exchanger designed based on round pins and the second for a heat exchanger based on drop-shaped pins. The two runs were done at the same Reynolds number equal to 2000 and the same meshing. After getting the results a path was drown following the nodes around the pin located at the 1st row and the 3rd line at mid height. The local heat transfer coefficient was plotted as in figure 12 versus the path length and as in figure 13 versus the angle theta. Theta starts from the stagnation point, follows the path around the pin and comes back to the stagnation point making 360 degrees.

Figure 13 shows that the drop shaped pin has around 50% more wetted surface area. This extra wetted surface area will allow increasing the heat flux and the heat transfer coefficient.

Figure 14 shows the second reason for the increased heat transfer coefficient of the drop shaped over the round pin. Down stream the round pin, the heat transfer coefficient was almost zero for an angle as big as 200 degrees due to separation, which disconnect the flow streamlines and detach the flow from the back pin surface. As a result the back pin surface will get hot and no heat

will be conducted by convection allowing the heat transfer coefficient to get small. In the same region and especially when we overlap the pins the flow streamlines get squeezed between the pins which force them to reattach to the pin surface after separation and thereby continue to exchange heat with the heated pin.

As a result the average heat transfer coefficient for the entire pin was calculated. The round pin in this case yielded $644.5\,W/m^2K$ for the heat transfer coefficient, while the drop pins yielded $882.4\,W/m^2K$ with an increase of 37%, which is in agreement with the total heat transfer improvement calculated from figure 11 for the same Reynolds number.

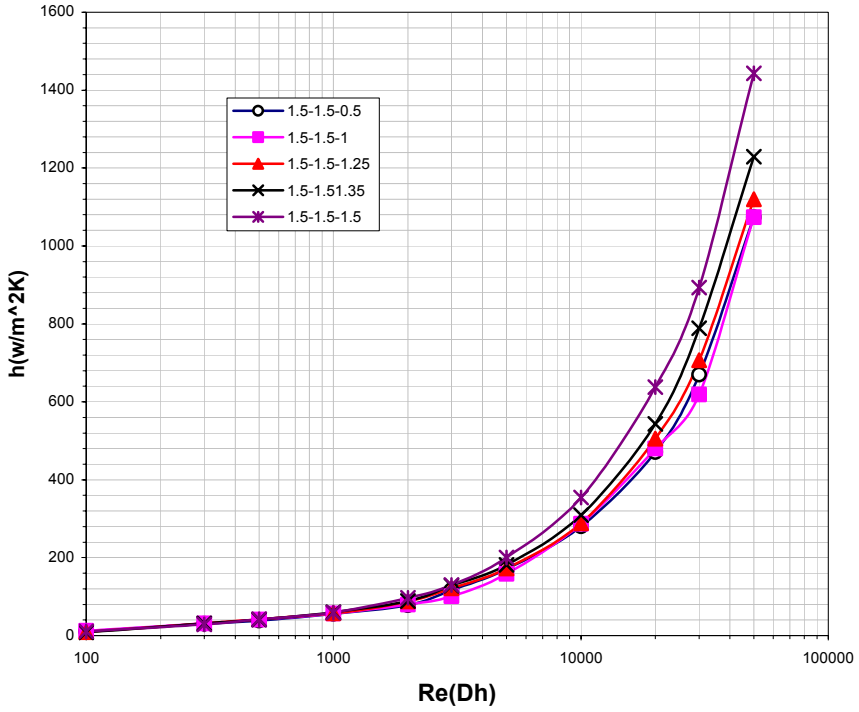

Figure 12. Heat transfer coefficient vs. Re for 1.5-1.5 configuration with different tail length

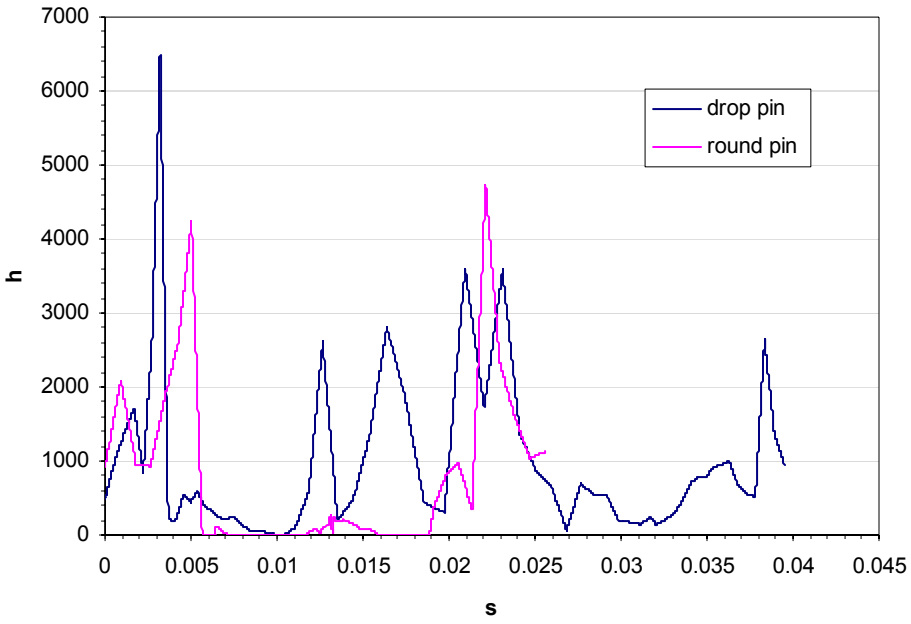

Figure 13. Heat transfer coefficient versus s (path around the pin) calculated around the pin located at 1st row, 3rd line at z=H/2 for the 1.5-1.5 configuration for drop and round pin.

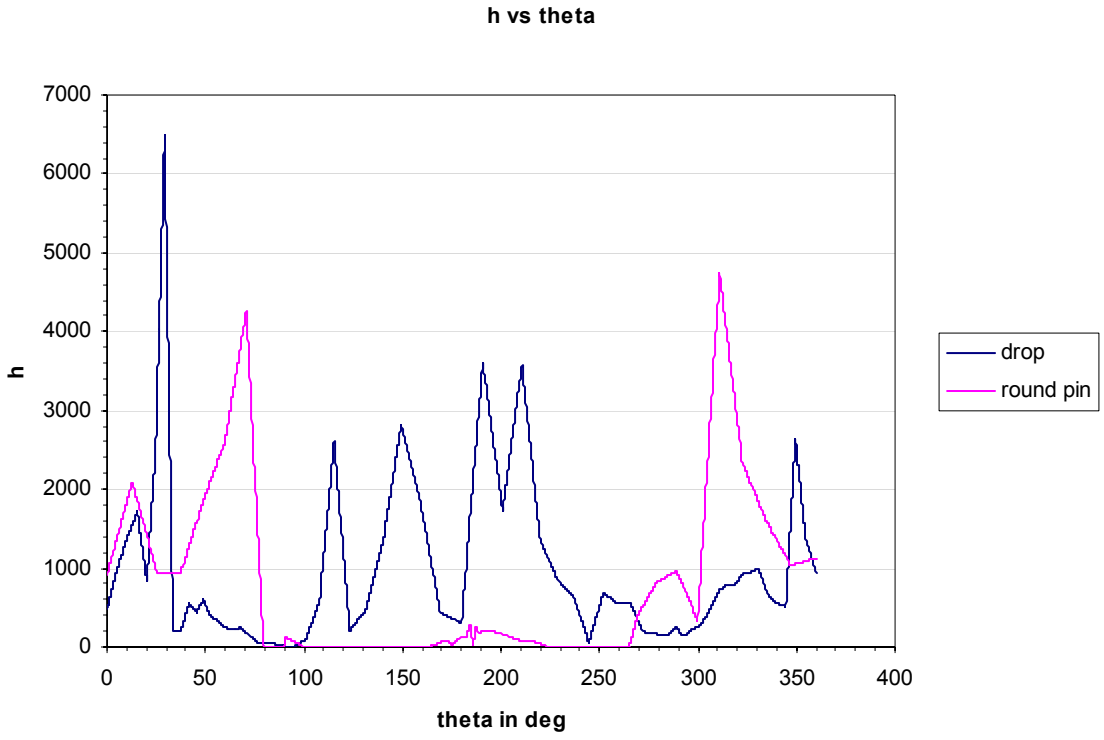

Figure 14. Heat transfer coefficient versus theta (angle around the pin starting at the stagnation point) calculated around the pin located at 1st row, 3rd line at z=H/2 for the 1.5-1.5 configuration for drop and round pin.

A path was drawn around each of the 10 central pins at mid height. The local heat transfer coefficient was calculated and averaged to find the average heat transfer coefficient for each pin at elevation of H/2. The average heat transfer coefficient was plotted versus X/L for both the drop and the round pins as shown in figure 15.

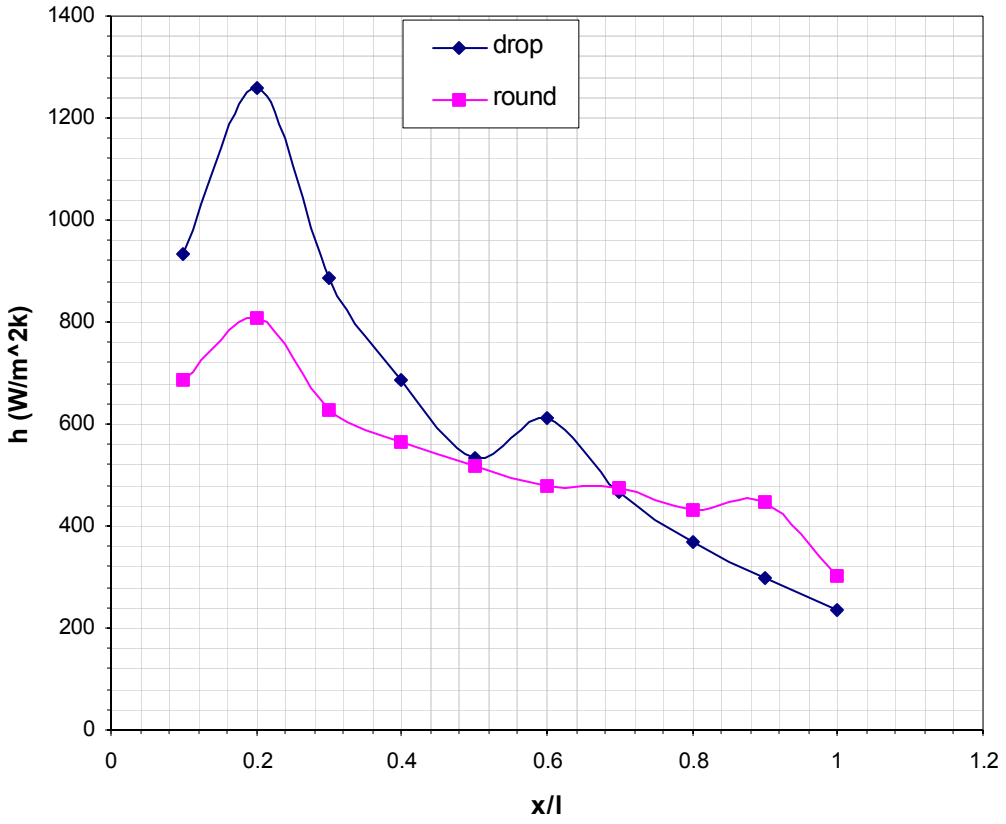

Figure 15. Comparison between the pins numerical heat transfer coefficient calculated around the central pins at height of z=H/2 versus the CH length for S/D=1.5-X/D=1.5 for the drops and the round pins.

Figure 15 shows that the drops give higher heat transfer coefficients than the round pins from row 1 to row 7. Starting from row 7 the round pins seem to be more efficient. The pin shape seems to have no big influence as we go far downstream.

Table 3 shows a comparison between the drops and the round pins heat transfer coefficients for the 10 selected pins.

Pin number	H(W/m^2K)round	H(W/m^2K)drop	%difference
1	686	932	35.8601
2	809	1260	55.7478
3	627	887	41.4673
4	563	688	22.2025
5	518	533	2.8958
6	480	613	27.7083
7	475	468	-1.474
8	430	368	-14.419
9	447	297	-33.557
10	303	236	-22.112

Table 3. Comparison between the drops and the round pins Numerical heat transfer coefficient calculated at the mid height of the 10 central pins.

The average improvement in heat transfer coefficient is about 17.7% for the entire 10 pins selected. Table 3 shows that having 7 rows instead of 10 can further enhance this improvement to 29.4% which is an important conclusion from a design point of view.

d. Velocity Profile

The velocity profile inside the test section was plotted in Figures 16 and 17 for both heat exchangers made of round pins and drops using the same scale. The same Reynolds number was used for both runs while the entrance velocity came very close for both runs.

These two figures explain the possible reason for the increase in the heat transfer coefficient of the drop

over the round pins. The round pins seem to have a wider separation region in the back, marked by a very small velocity indicating the discontinuity of the flow streamlines and the circulation of the flow downstream of the pins. This problem was solved by changing the pin geometry and more importantly by overlapping the pins using a long tail for the drops. By overlapping the drops as shown in Figure 15 the flow separates for a very short period of time and return to re-attach to the pin after being squeezed between the pins. The overlapping decreases the space between the pins, creates a nozzle effect due to the angular shape of the pin tail causing the flow to accelerate and to collide with the subsequent row of pins. The coalescence and interaction resulting in considerable acceleration of the flow between the neighboring pins of this flow in the drop pins case is the mechanism responsible for creating a more turbulent flow, leading to an increased heat transfer.

Another main advantage in delaying the separation and in reattaching the flow after the separation is the decrease in the pressure drop mainly due to frication drag in the case of the drop pins. This proves the decrease in friction factor shown in section (3.B.1) for the drop case.

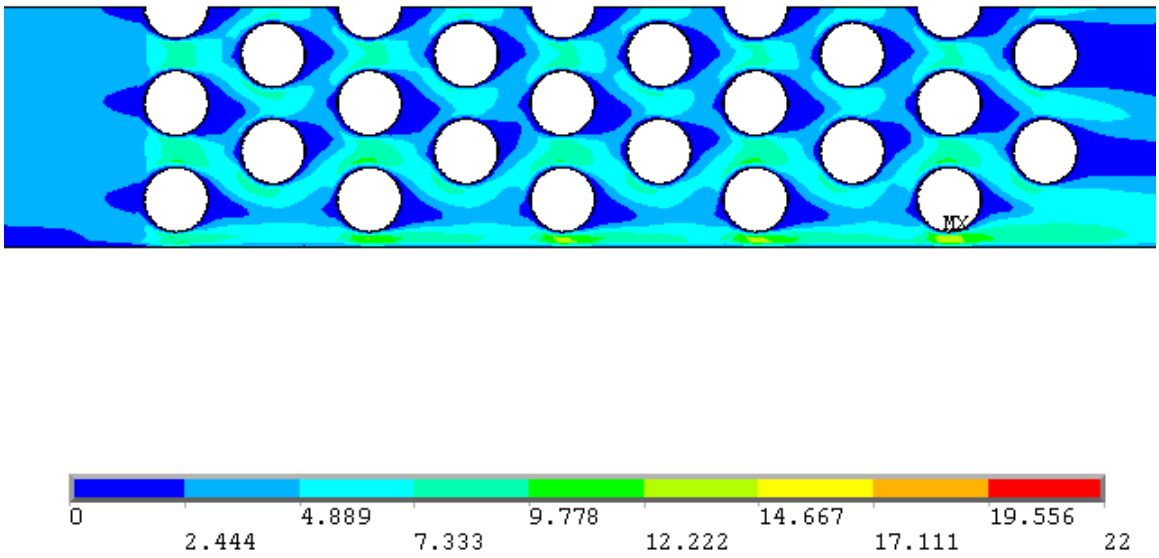

Figure 16. velocity profile for round pin HE at Re=20000

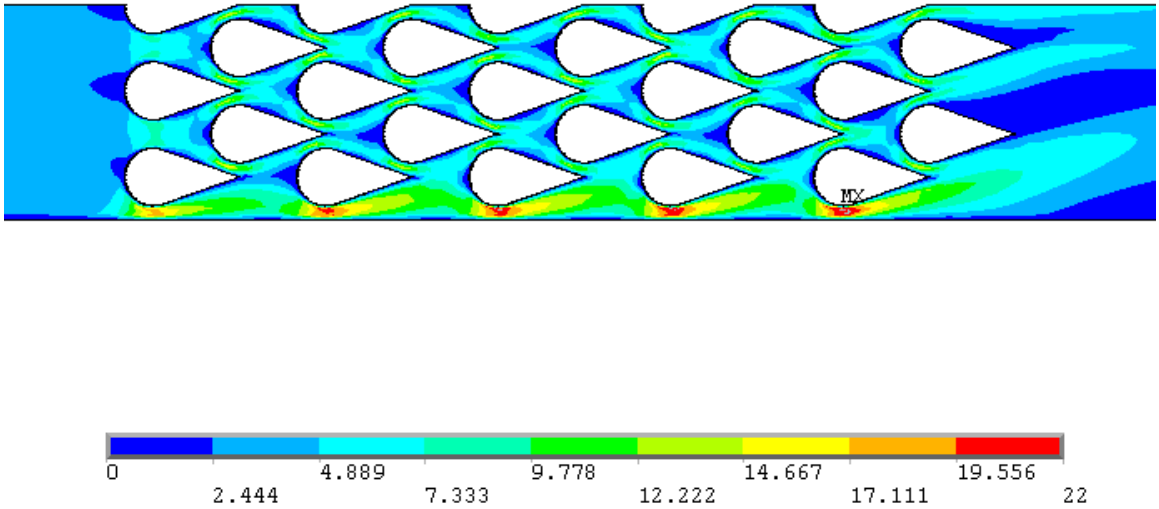

Figure 17. Velocity profile for drop pin HE at Re=20000 configuration1.5-1.5-1.5

d. Optimization

The heat transfer behavior alone does not provide a complete evaluation of heat exchanger

performance. The increase in pressure drop, which is a measure of the energy required by the system, must be weighed against the improvements of heat transfer for each pin fin configuration. This optimization process is critical for improving energy efficiency and comparing the contrast between heat exchanger gains and losses.

Kays and London (1984) show that an interesting and important feature of the compact heat exchanger performance can be demonstrated if the heat transfer coefficient based on the wetted surface area is plotted as function of the mechanical power expended to overcome the fluid friction, which is the friction power, per unit surface area.

Figure 18 shows the heat transfer coefficient plotted versus the friction power, both found numerically, for the configuration of X/D=1.5, S/D=1.5 and a different drop tail length. Obviously the configuration having L/D=1.5 has the highest heat transfer coefficient per unit friction power for the range of Reynolds numbers between 10000 and 50000. For Reynolds numbers less than 1000 the L/D=1.5 configurations still have better heat transfer coefficients than the round pins but are less efficient than the L/D=1.25 configuration. With this later observation and the fact that the L/D=1.5 configuration has a 16.77% increase in the wetted surface area over the round pins, the drops seem to achieve a significant improvement in the heat transfer over the round pins.

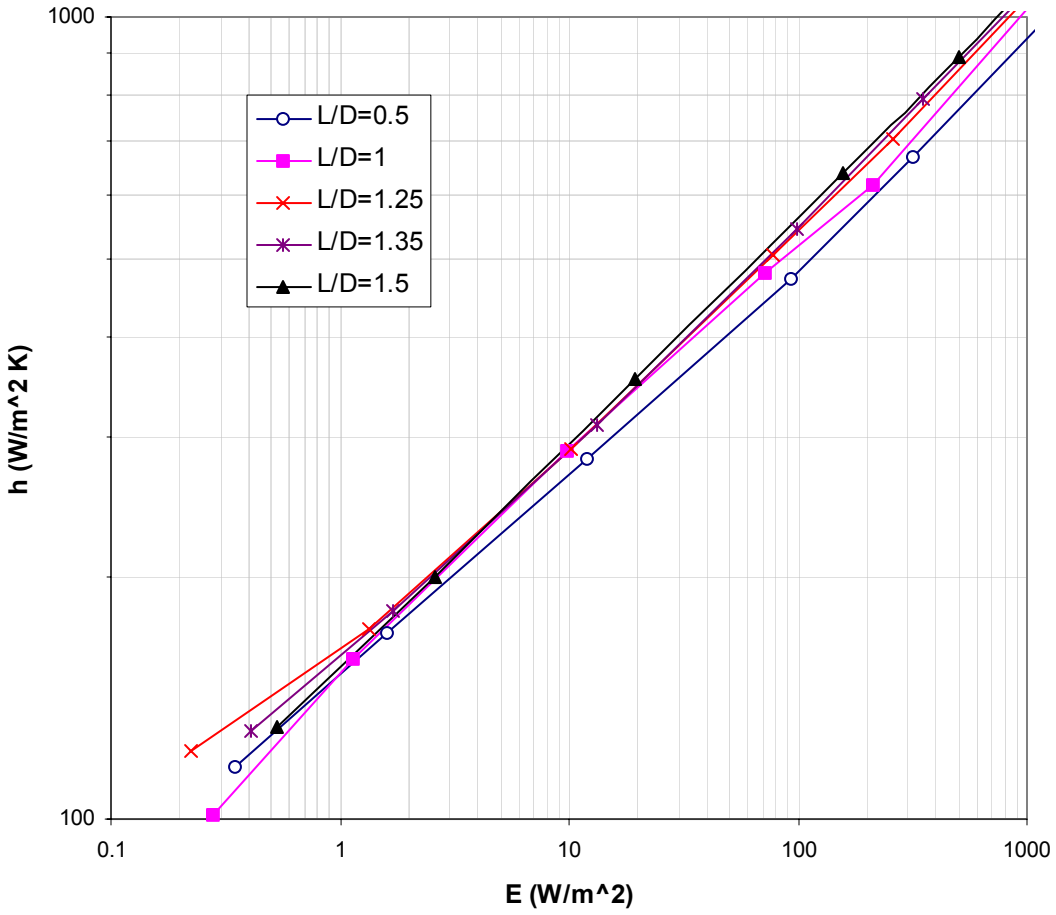

Figure 18. Comparison between the numerical heat transfer coefficient versus the friction power for X/D=1.5-S/D=1.5 with different drop tail length

To have a better picture of the advantage of changing the pin shape from round to drop, the heat transfer coefficient was plotted versus the friction power for a certain Reynolds number with different drop pin dimensions as shown in Figure 19 and 20.

Only the two extreme Reynolds numbers, 3000 and 50000, were selected for the sake of brevity.

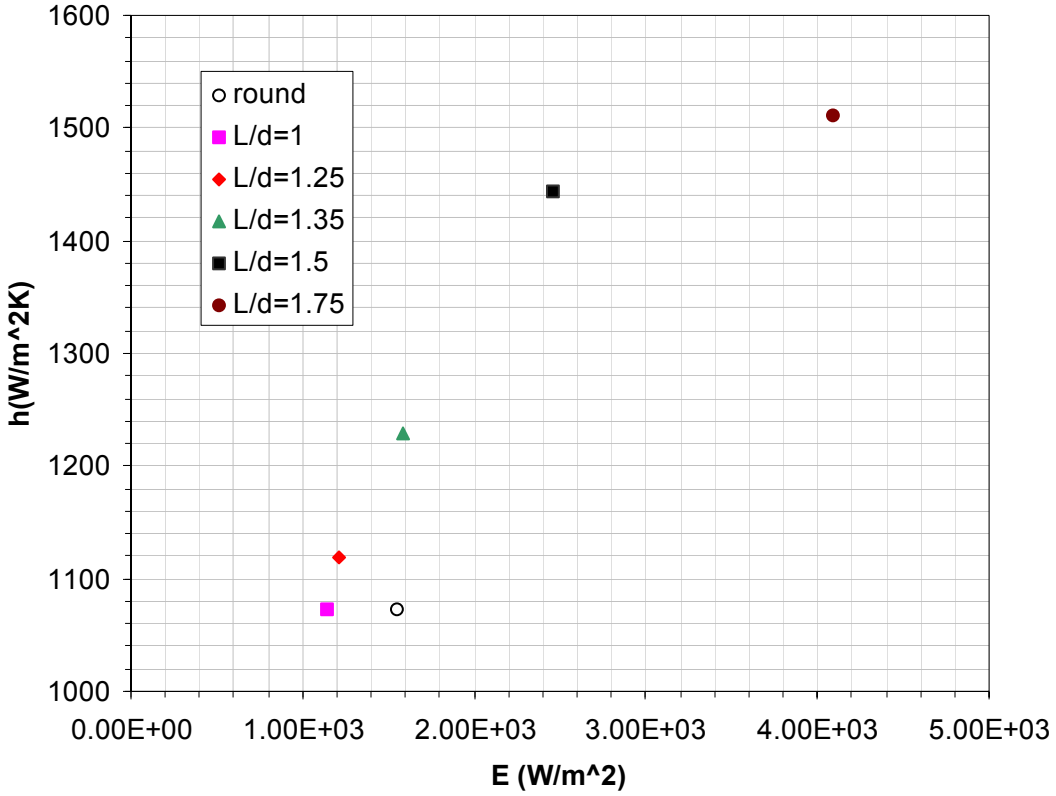

Figure 19. Numerical heat transfer coefficient versus the friction power at Re=50000 for X/D=S/D=1.5 and different drop size.

In Figure 19 at the Reynolds number of 5000, if we changing the pin shape from round to drop with L/D=1, we can have the same heat transfer coefficient with a decrease of 25.8% in friction power. At the same Reynolds number and for the same friction power, we can increase the heat transfer coefficient by 14.53% if we change the round pins to drop pins with L/D=1.35.

The heat transfer coefficient can be increased by 34.5% through changing the round pins to drops with L/D=1.5 but at the same time the friction power increases by 58%.

For L/D>1.5 the increase of heat transfer becomes very expensive from the viewpoint of friction power.

A similar behavior can be seen in Figure 20 with a Reynolds number of 3000 but with different rates of change.

These graphs lead to important conclusions regarding the CHE performance and design that it is possible to increase the heat transfer coefficient for the same friction power, or have the same heat transfer coefficient for lower pumping costs by streamlining the pin shape.

If the designer needs larger heat transfer rates the tail length can be increased leading to a much higher heat transfer coefficient for a modest increase in the friction power. however it is important to not exceed a certain critical tail length beyond which the increase in heat transfer is achieved at great expense.

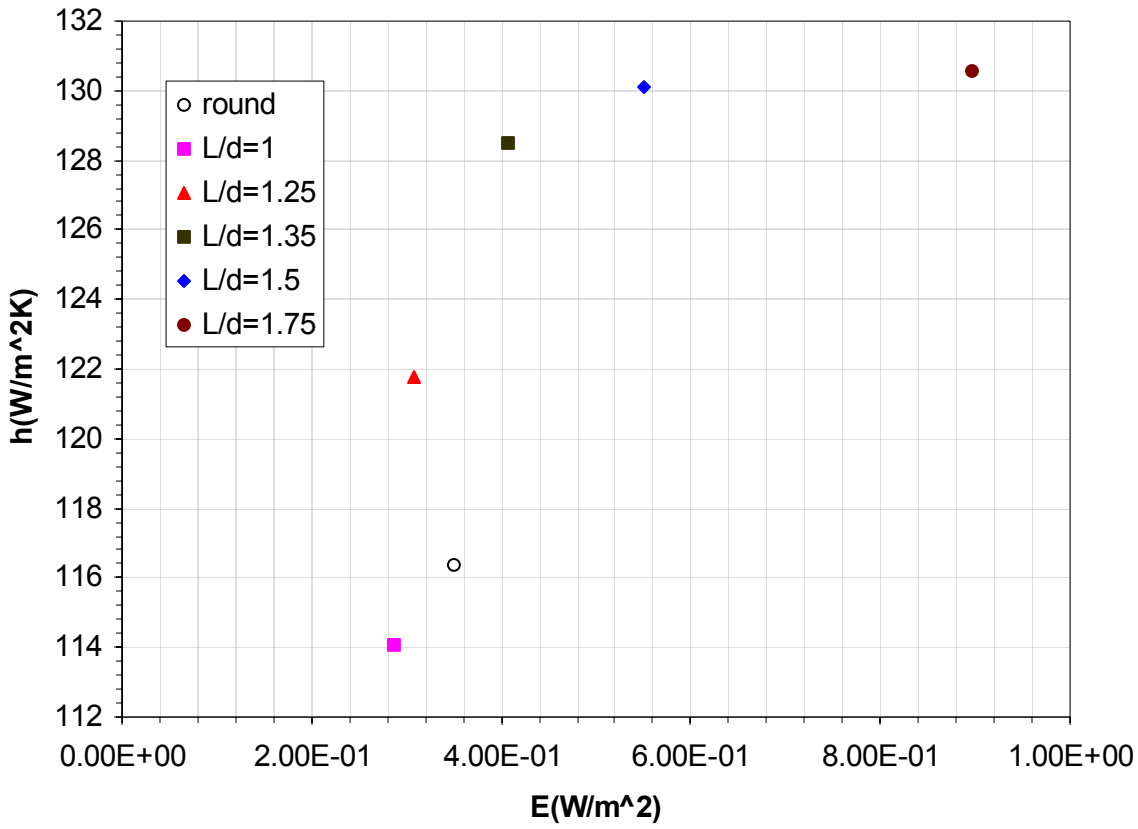

Figure 20. Numerical heat transfer coefficient versus the friction power at Re=3000 for X/D=S/D=1.5 and different drop size.

This behavior can be explained by noting that

- By changing the pin shape from round to drop, there is an increase in the wetted surface area to exchange heat with the flow, which increases the total heat transfer rate.
- By having a tail in the drop case the separation is delayed which leads to decrease in the friction drag and power.

- By overlapping the drops, the flow can be made to reattach after a short period of separation by being squeezed between the pins.
- The overlapping also creates a nozzle effect due to the angular shape of the pintail causing the flow to accelerate and collide with the subsequent row of pins. The interaction of the pins and the accelerating flow together with the coalescence lead to more turbulence, which help to increase the heat transfer.
- After L/D=1.5 the increase in heat transfer is accompanied by a large increase in the friction factor, due to a decrease in the empty space between the pins making it hard for the fluid to follow the flow passages resulting in an increase in the frictional losses.

C. EXPERIMENTAL RESULTS

1. Drop Shaped Pins: Experimental vs. Numerical Results

To check the validity of non-dimensionalizing with respect to the hydraulic diameter a scaling analysis was conducted. The check consisted of carrying out numerical runs for different values of X but a fixed configuration and compareing the non-dimensional results, which in this case are the Nusselt number and the friction factor. The dimensional analysis can be conducted by changing X to obtain scaled down CHE models that are similar. And by definition the flow conditions for model test are

completely similar if all relevant dimensionless parameters have the same corresponding values for the model and prototype.

The Table below shows the Nusselt number and the friction factor for different similar models and for the 1.5-1.5-1.25 configuration at the Reynolds number of 20000.

X(m)	Nu	f
0.006	141.63	0.68
0.0127	140.98	0.69
0.02	140.83	0.69
0.03	141.14	0.7
0.06	142.59	0.71

Table 4. Nusselt number and Friction factor for similar heat exchanger models.

This table shows that the maximum difference in the Nusselt number between all the studied models is about 1.2% while the maximum difference in the friction coefficient is about 4.2% which is acceptable. This similarity check allows experimental and numerical results to be compared for all continuum length scales regardless of the actual dimensions of the heat exchanger.

a. Nusselt Number

In Figure 21 the numerical as well as the experimental Nusselt number were plotted versus the Reynolds number for the same 1.5-1.5-1.5 configuration. Readily seen is a good agreement between the two Nusselt number as the Reynolds number ranges between 3000 and

around 20000, where the error extends up to 18%. After a Reynolds number of 2000 the numerical and experiment data start to diverge and the error starts to increase. This observation is important, since it allows trust in the ANSYS model knowing that most applications of interest range in Reynolds numbers from [3000,20000].

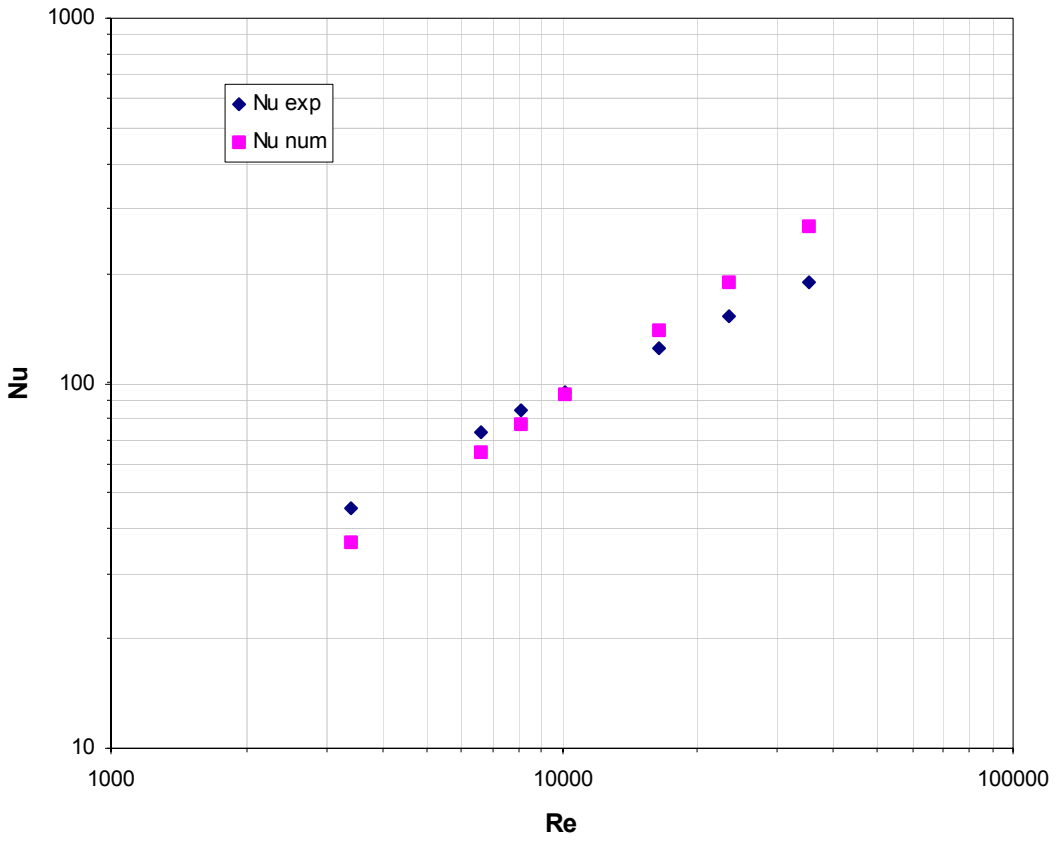

Figure 21. Comparison between numerical and experimental results for the drops Nusselt number for the case of X/D=1.5-S/D=1.5-L/D=1.5

b. Friction Factor

Figure 22 shows the numerical friction factor predicted based on the ANSYS model for the configuration

1.5-1.5-1.5 with x=0.0127m and the experimental friction factor calculated for the same configuration with x=0.05m based on the experimental results.

From this graph the numerical model has evidently over predicted the frication factor. The numerical model estimated that the friction is almost independent of the Reynolds number and stays constant around a value of 1 for the Reynolds number range of 3000 to 30000. This behavior of friction factor could be expected in the case of rough ducts which however is not true in our study. The experimental data shows that the friction factor is much less than that predicted with the numerical model with the error ranges between 39 and 71%.

The reason for this error could be a failure in the turbulent model to predict the flow behavior inside the heat exchanger,which can be proved based on Figure 14. For the case of round pins in turbulent flow, the streamlines are known to separate at an angle of 108 degrees around the pin. However back in Figure 13 the separation occurs at an angle of 80 degrees even for the first row where no other pins are interacting with the flow. The same figure also shows that the drop pins separate before the round pins, which contradicts with the fluid mechanics principles.

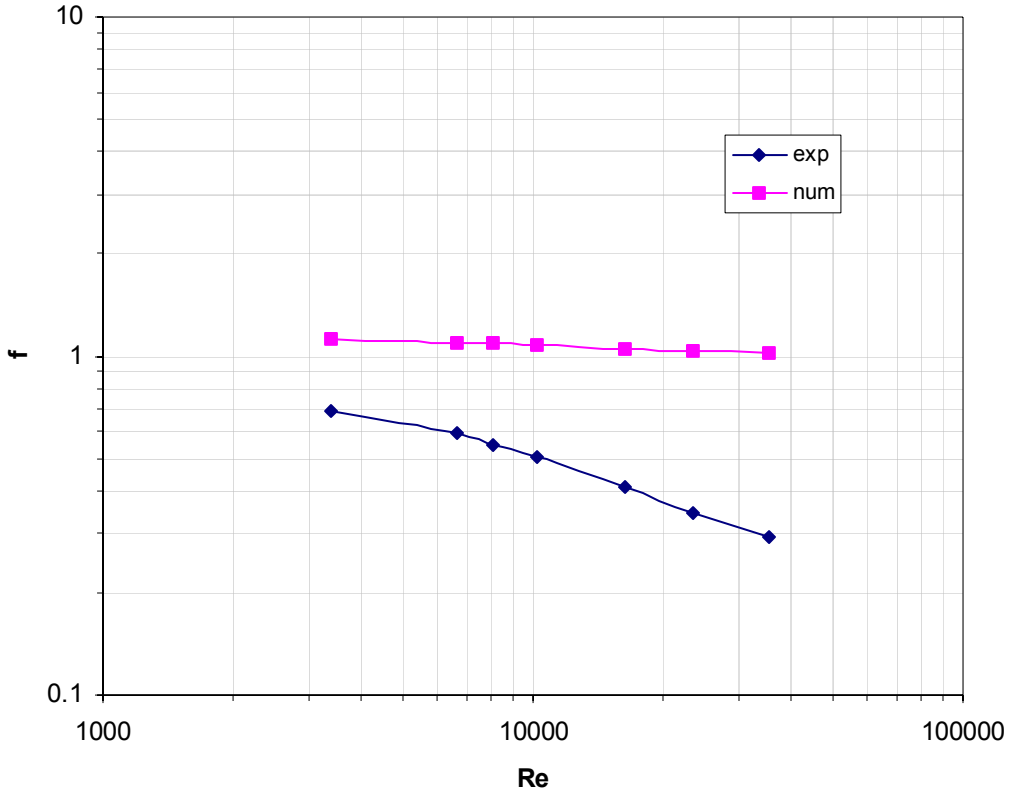

Figure 22. Comparison between numerical and experimental results for the drops friction factor for the case of X/D=1.5-S/D=1.5-L/D=1.5

2. Drop vs. Round Pins: Experimental Results

a. Heat Transfer Coefficient

In Figure 23 the experimental heat transfer coefficient for the round pins CHE (configuration 1.5-1.5) and the round pins CHE (configuration 1.5-1.5-1.5) were plotted versus the Reynolds. A measurable improvement for the same Reynolds number was realized by changing the pin shape from round to drops. This improvement was calculated to be between 33% for low Reynolds numbers to 16% for high Reynolds numbers. The reason for this improvement is as was

discussed in B.3.b the increase of the wetted surface area due to the long drop tail adding an extra wetted surface are. The overlapping of the pins, which allows the flow to be squeezed, to be accelerated between the pins and to be forced to reattach again to cool the pin surface. The overlapping also decreases the space between the pins, which creates a nozzle effect due to the angular shape of the pin tail. This causes the flow to accelerate and collide with the subsequent row of pins, negotiating the flow interaction around the pin with an adjacent accelerating flow creating more turbulence.

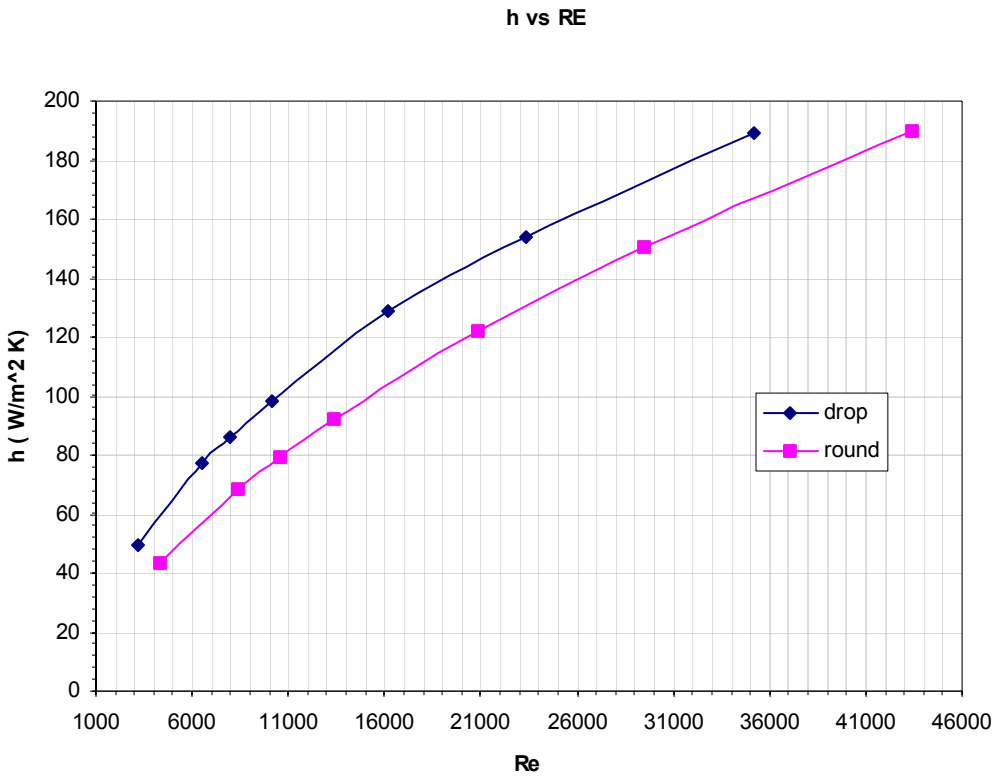

Figure 23. Comparison between the experimental heat transfer coefficient for the drop-shaped and round pins (Ramthun, 2002) versus Re.

b. Friction Factor

Figure 24 shows the experimental friction factor for the round pins CHE (configuration 1.5-1.5) and the round pins CHE (configuration 1.5-1.5-1.5) plotted versus the Reynolds. It can be clearly seen that the drop-shaped HE has a much smaller friction factor than the round pins HE. This decrease ranges between 20% for low Reynolds number and 50% for high Reynolds numbers. The reason for this improvement could be as explained by delay in the flow separation down stream the pin and the reattachment in drop pins case causing the form drag to goes down.

.

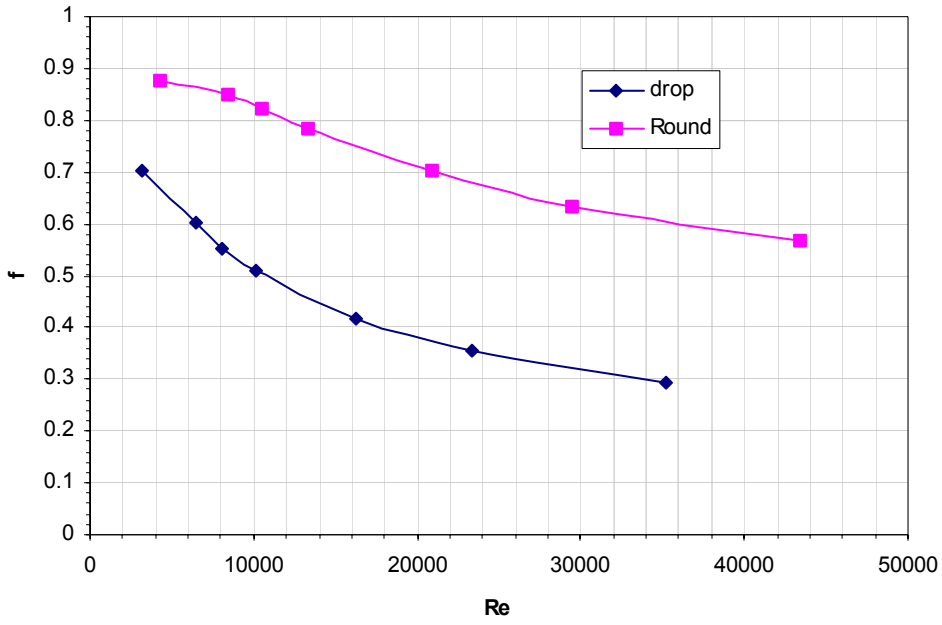

Figure 24. Comparison of experimental results for the friction factor for drop-shaped pins from the current study with round pins (Ramthun, 2003).

c. Optimization

As discussed before, neither the heat transfer behavior nor the friction factor alone could provide a complete evaluation of the heat exchanger performance. The heat exchanger performance demonstrated and compared in Figure 25, which plots the heat transfer coefficient based on the wetted surface area as function of the mechanical power expended to overcome the fluid friction, which is the friction power per unit surface area.

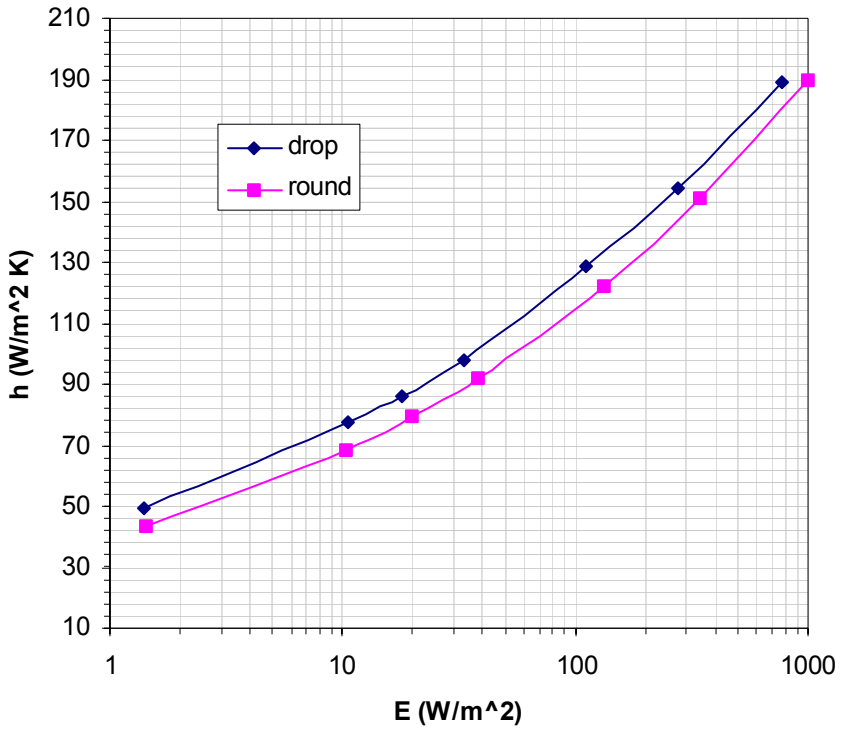

Figure 25. Experimental Heat transfer coefficient for the drop-shaped and round pins CHE versus the friction power.

Figure 25 shows that for all the range of Reynolds number investigated, the CHE, made of drop pins,

has an improved heat transfer coefficient for the same friction power expended to overcome the fluid friction. This improvement was calculated to be around 16% for low Reynolds numbers to 9% for high Reynolds number as shown in Table 5.

E (W/m^2)	h (W/m^2K) (round pins)	h (W/m^2K) (drops)	% difference
1.41	43	50	+16.28
5	58	67	+15.5
10.45	77.5	68.5	+13.13
100	116	130	+12
200	134	147	+9.7

Table 5. Rate of improvement of the experimental heat transfer coefficient of the drops (configuration 1.5-1.5-1.5) over the round pins (configuration 1.5-1.5) for the same friction power.

Table 5 shows that for the same friction power the drops have around 16% improvement in the heat transfer coefficient for low Reynolds numbers and around 10% for high Reynolds numbers. Also the drops have a higher wetted surface area than the round pins allowing the increase of heat flux Q to be higher than 16%.

THIS PAGE INTENTIONALLY LEFT BLANK

V. CONCLUSIONS AND RECOMMENDATIONS

A. CONCLUSIONS

A 3-D numerical simulation was conducted to evaluate the performance of a compact heat exchanger made of drop shaped pin fins. The primary task was to vary the pins spacing in the span wise and stream wise direction to select the optimum configuration giving the highest heat transfer for a certain pressure drop. The next task was to vary the drop tail and select the best drop dimensions capable of increasing the heat transfer while keeping the same friction power. Recent experimental work was conducted to evaluate the accuracy of the numerical work. A comparison between the drops and the round pins was conducted to evaluate the improvement in heat transfer and pressure drop by changing the pin shape.

The numerical results indicated that

- X/D=1.5, S/D=1.5,L/D=1.5 is the optimum HE configuration.
- The drop shaped pin fins yield a considerable improvement in heat transfer compared to circular pin fins for the same pressure drop characteristics. The main reasons that explain this are as follows:
  - The drops have a higher wetted surface area leading to a higher heat flux
  - The drop shape forces the separation to delay
  - Overlapping the drops, the flow was forced to reattach after separation and to accelerate between the pins creating a nuzzle effect and increasing the turbulence.

- The drops have a considerable decrease in the friction factor in comparison with the round pins.

The experimental results indicated the following:

- The drops give a higher heat transfer than the round pins for the same friction power.
- The drops lead to a considerable decrease in the friction power in comparison to the round pins.
- An agreement between the numerical Nusselt number and the experimental Nusselt number for Reynolds number ranged between 3000 and 20000. after 20000 the difference start to become high.
- The experimental friction factor seems to be much lower than the numerical one and ANSYS seems to overestimate the friction factor.

B. RECOMMENDATIONS

A unit cell analysis of the CHE in Appendix B shows that increasing the ratio H/D could have a big influence on the wetted surface area and as a result a big influence on the heat transfer rate. So investigating the influence of H/D could be the next step in a future study.

A discrepancy was discovered in the numerical and experimental friction factors. Future studies could consider improved turbulent models to reduce this error.

Finally, other pin shapes could have better performance than round pins and drop pins and could be investigated.

APPENDIX A. NUMERICAL ACCURACY

A. MESH

Since the current license of ANSYS 6.0 is limited to 256,000 nodes, two runs were done for each configuration at a certain Reynolds number. The first one was completed at a number of nodes close to 256,000 and the second at around 25-30% less nodes. A run is considered grid independent if the overall heat transfer rate difference between the two remains below 2%.

B. NUMBER OF ITERATIONS

A run is valid if the difference between the heat transfer rate for the last 10-iterations is less than 2%. It typically required 230 iterations to achieve convergence. If not, additional iterations were carried out as necessary.

C. OUTLET TEMPERATURE

The outlet temperature was calculated using equation 1.6 and compared to the one provided by the ANSYS result file. For a run to be valid the difference between the two was required to be less that 0.1 K.

THIS PAGE INTENTIONALLY LEFT BLANK

APPENDIX B. UNIT CELL ANALYSIS OF HEAT EXCHANGER LAYOUT

A. GENERAL DIMENSIONS

- Overall heat exchanger length $l = N_x x + L$ with N_x = number of rows in the streamwise direction.
- Overall heat exchanger width $W = N_s S$ with N_s number of rows in the spanwise direction.
- H: unit cell height
- Total unit cell height= M*H with M being the number of layers.
- $A_{fp} = Wl$ Foot print area.
- $A_f = WMH$ Frontal flow area.

B. STAGGERED ARRAY PATTERN OF DROP-SHAPED PINS

Limitations for a unit cell

- $S > D$
- $X \geq \frac{D}{2}\ x \geq \frac{D}{2}$
- $L < 2X - D/2$
- $\sqrt{X^2 + \left(\frac{S}{s}\right)^2} < D$

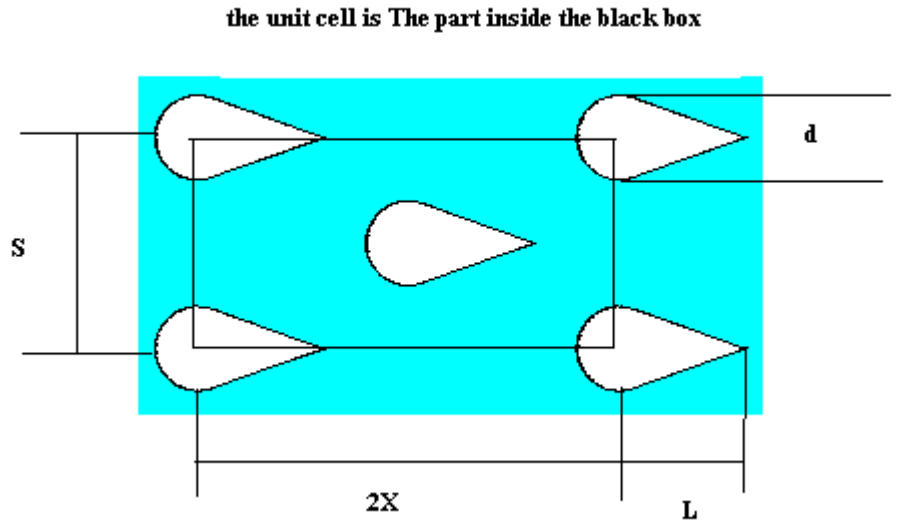

Figure 26. General form of drops Unit cell.

C. UNIT CELL PROPERTIES AND CALCULATIONS

- $V_t = SH2X$ Total unit cell volume
- $V_0 = V_t - 2\left[\frac{D}{2}L\cos\theta + \frac{\pi D^2}{4}\frac{\pi + 2\theta}{2\pi}\right]H$ Unit cell open volume
- Unit cell wetted surface area
- $D_h = \frac{4V_0}{A_w}$ Unit cell hydraulic diameter
- Porosity of the unit cell

$$\varepsilon = \frac{V_0}{V_t} = 1 - \frac{\frac{D}{2}[L\cos\theta + \frac{\pi D}{2}\frac{\pi + 2\theta}{2\pi}]H}{XSH}$$

$$\varepsilon = 1 - \frac{1}{2}[(\frac{D}{X})(\frac{D}{S})(\frac{L}{D}\cos\theta + \frac{\pi + 2\theta}{4})$$

- Volumetric heat transfer area density of the unit cell $\alpha = \frac{A_w}{V_t} = \frac{A_w}{V_0}\frac{V_0}{V_t} = \frac{4}{D_h}\varepsilon$

Given an area density, the total heat transfer area could be found from $A_w = \alpha V_t$ was $V_t = A_{fp} H$.

$\alpha H = \frac{A_w}{A_{fp}}$ this equation is very important because it shows that to increase the wetted surface area for the same foot print area, we need to have high H or high α.

$$\alpha H = \frac{A_w}{A_{fp}} = 2 + 2[-\frac{D}{2} L\cos\theta + 2HL\cos\theta - \frac{(\pi + 2\theta)D^2}{8} + (\pi + 2\theta)\frac{DH}{2}]/(2XS)$$

$$\alpha H = 2 + \frac{4H - D}{XS}[\frac{L\cos\theta}{2} + \frac{(\pi + 2\theta)D}{8}]$$

$$\alpha H = 2 + 4(\frac{H}{D} - \frac{1}{4})[\frac{D}{X}\frac{D}{S}(\frac{L}{D}\cos\theta + \frac{\pi + 2\theta}{4})\frac{1}{2}]$$

$$\alpha H = \frac{A_w}{A_{fp}} = 2 + 4(1 - \varepsilon)(\frac{H}{D} - \frac{1}{4})$$

The last equation relate two very important characteristic variable of heat exchanger, which are α and ε .

THIS PAGE INTENTIONALLY LEFT BLANK

APPENDIX C. SAMPLE NUMERICAL RUN

This appendix provides a sequence of how the numerical results were achieved.

The ANSYS result file provide us with the

- $\dot{m}$/4: The mass flow
- ΔP_T/4: The total pressure drop including the inlet and outlet pressure drop.
- T_{out}: The outlet temperature
- q/4:The heat conducted by the fluid in the test section
- The mass flow pressure drop and the heat transfer is found by multiplying this three parameter by 4. The pressure drop in the test section is found by subtracting the pressure drop due to friction in the inlet and outlet section. Knowing these data and the area wetted Aw, the open volume Vo, the total volume Vt, the hydraulic diameter Dh from geometry and the wall temperature Tw the following calculation is made:
- The log mean temperature

$$\Delta T_{LM} = \frac{(T_{wall} - T_{coolant_{in}}) - (T_{wall} - T_{coolant_{out}})}{\ln(\frac{T_{wall} - T_{coolant}}{T_{wall} - T_{coolantout}})}$$

- The heat transfer coefficient

$$\overline{h} = \frac{q}{A_{wetted}\Delta T_{LM}}$$

- The Reynolds number

$$\mathrm{Re}_{Dh} = \frac{\dot{m} D_h}{\mu \overline{A}}$$

- The Nusselt Number

$$Nu_{Dh} = \frac{\bar{h}\, D_h}{K}$$

- The average velocity

$$\bar{U} = \frac{\dot{m}}{\rho \bar{A}}$$

- The friction factor

$$f = \frac{2\Delta P D_h}{\rho(10x + L)\bar{U}^2}$$

- The friction energy

$$E = \frac{\dot{m}\Delta P}{\rho A_w}$$

These are the most important parameters. Finally the graphs of h versus E will be plotted to see the efficiency of each configuration.

APPENDIX D. SAMPLE EXPERIMENTAL RUN

This appendix provides a sequence of how the experimental results were achieved.

From the software results file the following data was collected:

- V_f: The flow meter output voltage used to calculate the mass flow
- $V_{\Delta P}$: The pressure transducer output voltage used to calculate the pressure drop inside the test section.
- V_{Pexit}: The pressure transducer output voltage measured after removing the pressure's transducer tube located at the entrance. This voltage is used to calculate the exit pressure.
- $V_{foffset}$: The voltage from the offset mass flow calculated during the zero flow test. This voltage is used to correct the mass flow for the rest of the runs.
- $P_{out} = P_{atm} - 249 \times 6.25(V_{pexit} - V_{\Delta Poffset})\, V_{\Delta Poffset}$: the offset voltage from the pressure transducer used to correct the pressure drop inside the test section as well as the exit pressure.
- P_{atm}: The atmospheric pressure as given by the NOAA website for Monterey.
- T_{in}: The inlet temperature.
- T_{out}: The outlet temperature calculated after averaging 4 exit temperatures read by 4 different thermocouples located at the exit.
- T_{wall}: The wall temperature is set to be constant for the whole set of runs.

Based on this set of data, the desired results are calculated as below

- ΔP : Pressure drop inside the test section is

$\Delta P = 249 \times 6.25(V_f - V_{foffset})$ The 6.25 used to convert the voltage to inH_2O and the 249 is to convert the inH_2O to Pascal.

- P_{out} : Pressure at the exit of the test section is

$P_{out} = P_{atm} - 249 \times 6.25(V_{pexit} - V_{\Delta Poffset})$

- ρ : The air density will be $\rho = \frac{P_{out}}{287 \times T_{out}}$

- υ : The kinematic viscosity is

$\upsilon = 0.0000171(\frac{T_{out}}{273})^{3/2}(\frac{273+110.4}{T_{out}+110.4})$

- $\dot{q}$: the volumetric mass flow is

$\dot{q} = 0.018868(V_f - V_{foffset})$

- $\dot{m}$: the mass flow is

$\dot{m} = \dot{q} \times \rho$

- Re: the Reynolds number is

- $\mathrm{Re} = \frac{\dot{m} \times D_h}{\rho \upsilon \times \overline{A}}$ $\mathrm{Re} = \frac{\dot{m} \times D_h}{\mu \times \overline{A}} = \frac{\rho \dot{q}}{\mu \times \overline{A}} D_h = \frac{P \dot{q}}{RT} \times \frac{LD_h}{\mu V_0}$

- $Nu = \frac{h \times D_h}{K}$ U_{avg} : The average velocity inside the test section will be

$U_{avg} = \frac{\dot{q}}{\overline{A}}$

- f: the friction factor is

$f = \frac{2\Delta P \times D_h}{(10X)\rho \times U^2_{avg}}$

- ΔT_{LM} : The log mean temperature

$$f = \frac{2\Delta P \times D_h}{(10X)\rho \times U^2_{avg}} = \frac{2\Delta P \times D_h \times R \times T}{(10X)P \times U^2_{avg}}$$

$$f = \sqrt{\left(\frac{\Delta(\Delta P)}{\Delta P}\right)^2 \times \left(\frac{\Delta T}{T}\right)^2 \times \left(\frac{\Delta P}{P}\right)^2}$$

$$\Delta T_{LM} = \frac{(T_{out} - T_{in})}{\ln(\frac{T_{wall} - T_{in}}{T_{wall} - T_{out}})}$$

- h :the heat transfer coefficient is

$h = \frac{Q_{net}}{A_w \Delta T_{lm}}$ With Q_{net} being the net heat flux calculated after subtracting the heat losses.

- Nu: the Nusselt number will be

$Nu = \frac{h \times D_h}{K}$ With K being the air conductivity and the value of 0.0264 used for the operational temperature.

- The friction energy is

$$E = \frac{\dot{m} \Delta P}{\rho A_w}$$

THIS PAGE INTENTIONALLY LEFT BLANK

APPENDIX E. ERROR ANALYSIS FOR EXPERIMENTAL RESULTS

A. REYNOLDS NUMBER

$$\mathrm{Re} = \frac{\dot{m} \times D_h}{\mu \times \overline{A}} = \frac{\rho \dot{q}}{\mu \times \overline{A}} D_h = \frac{P \dot{q}}{RT} \times \frac{LD_h}{\mu V_0}$$

The error in Reynolds number will be related to the 3 variables P T and $\dot{q}$ as below

$$\frac{\Delta \mathrm{Re}}{\mathrm{Re}} = \sqrt{(\frac{\Delta P}{P})^2 + (\frac{\Delta T}{T})^2 + (\frac{\Delta \dot{q}}{\dot{q}})^2}$$

$$\frac{\Delta \mathrm{Re}}{\mathrm{Re}} = \sqrt{(\frac{\Delta P}{P})^2 + (\frac{\Delta T}{T})^2 + (\frac{\Delta \dot{q}}{\dot{q}})^2}$$

B. NUSSELT NUMBER

Same procedure as above was utilized to calculate the error in Nusselt Number.

The error in Nusselt number is related to the error in the heat transfer coefficient. The error in heat transfer coefficient is related to the error in heat flux Q calculated during the experiment and the ΔT_{LM} as shown in the following equations.

$$Nu = \frac{h \times D_h}{K} \qquad h = \frac{Q_{net}}{A_w \Delta T_{lm}}$$

The error in q will be related to the on and off time calculated for the heaters.

$$\frac{\Delta Nu}{Nu} = \frac{\Delta h}{h} = \sqrt{(\frac{\Delta t}{t})^2 + (\frac{\Delta T}{\Delta T_{LM}})^2}$$

C. FRICTION FACTOR

$$f = \frac{2\Delta P \times D_h}{(10X)\rho \times U^2_{avg}} = \frac{2\Delta P \times D_h \times R \times T}{(10X)P \times U^2_{avg}}$$

$$f = \sqrt{\left(\frac{\Delta(\Delta P)}{\Delta P}\right)^2 \times \left(\frac{\Delta T}{T}\right)^2 \times \left(\frac{\Delta P}{P}\right)^2}$$

LIST OF REFERENCES

Arora,S.C, Abdel Messeh,W., "Pressure Drop And Heat Transfer Characteristics Of Circular and Oblong Low Aspect Ratio Pin Fins", Pratt & Whitney Canada INC., Longueuil, Quebec, J4K 4X9, Canada.

Chen, Z., Li, Q., Meier, D., Warnecke, H.J., "Convective Heat Transfer and Pressure Loss in Rectangular Ducts with Drop-Shaped Pin Fins", Journal of Heat and Mass Transfer, Vol. 33, pp. 219-224, 1997.

Chen, Z., Li, Q., Flechtner, U., and Warnecke, H.J., "Heat Transfer and Pressure Drop Characteristics in Rectangular Channels with Elliptic Pin Fins," *Int. J. of Heat and Fluid Flow*, Vol 19, 1998, pp. 245-250.

Chyu, M. K., "Heat Transfer and Pressure Drop for Short Pin-Fin Arrays with Pin-End Wall Fillet", Presented at the Gas Turbine and Aeroengine Congress and Exposition-June4-8, 1989, Toronto, Ontario, Canada.

Chyu, M. K., Goldstein, R. J., "Influence of an Array of Wall-Mounted Cylinders on the Mass Transfer from a Flat Surface.", International Journal of Heat and Mass Transfer, vol. 34, pp.2175-2186, 1991.

Chyu, M. K., Hsing, Y. C., Shih, T. I.-P., Natarajan, V., "Heat Transfer Contributions of Pins and End Wall in Pin-Fin Arrays: Effects of Thermal Boundary Condition Modeling", Journal of Turbomachinery, vol. 121, pp. 257-263, 1999.

Donahoo, E. E., Camci, C., Kulkarni, A. K., Belegundu, A. D., "Determination of Optimal Row Spacing for a Staggered Cross-Pin Array in a Turbine Blade Cooling Passage", Enhanced Heat Transfer, vol. 8, pp. 41-53, 2001.

Kays, W. M., Crawford, M. E., *Convective Heat and Mass Transfer,* 3rd ed., McGraw-Hill, Inc., 1993.

Kays, W. M., London, A. L., "Compact Heat Exchangers", McGraw-Hill, Inc., 1984.

Metzger, D. E., Berry, R. A., Bronson, J. P., "Developing Heat Transfer in Rectangular Ducts with Staggered Arrays of Short Pin Fins", Journal of Heat Transfer, vol. 104, pp. 700-706, 1982.

Metzger, D. E., Fan, C. S., Haley, S. W., "Effects of Pin Shape and Array Orientation on Heat Transfer and Press Loss in Pin Fin Arrays", Journal of Engineering for Gas Turbines and Power, vol. 106, pp. 252-257, 1984.

Shah, R. K., Kraus, A. D., Metzeger, D., "Compact Heat Exchangers", Hemispheric Publishing Corporation, 1990.

Tahat, M. A., Babus'Haq, R. F., Probert, S. D., "Forced Steady-State Convections from Pin-Fin Arrays", Applied Energy, vol. 48, pp. 335-351, 1994.

VanFossen, G. J., "Heat-Transfer Coefficients for Staggered Arrays of Short Pin Fins", Journal of Engineering for Power, vol.104, pp. 268-274, 1982.

Ramthun, D, "An Experimental Study of a Pin Fin-Heat Exchanger", Master's Thesis, Naval Postgraduate School Monterey, California, 2003.

INITIAL DISTRIBUTION LIST

1. Defense Technical Information Center
   Ft. Belvoir, VA

2. Dudley Knox Library
   Naval Postgraduate School
   Monterey, CA

3. Professor Ashok Gopinath, Code ME/Gk
   Department of Mechanical Engineering
   Naval Postgraduate School
   Monterey, CA

4. Professor Young W. Kwon ME/KW
   Department of Mechanical Engineering
   Naval Postgraduate School
   Monterey, CA

5. Jeffery Summer
   Department of Mechanical Engineering
   Naval Postgraduate School
   Monterey, CA

6. Jui Sheng Choo
   Department of Mechanical Engineering
   Naval Postgraduate School
   Monterey, CA

7. Mechanical Engineering Program Officer (Code 74)
   Naval Postgraduate School
   Monterey, CA